

STEM CELL MEMBRANE ENGINEERING: AN APPROACH FOR
MODULATING CELL-BIOMATERIAL INTERACTIONS

BY

NIDHANJALI BANSAL

THESIS

Submitted in partial fulfillment of the requirements
for the degree of Master of Science in Bioengineering
in the Graduate College of the
University of Illinois at Urbana-Champaign, 2014

Urbana, Illinois

Adviser:

Assistant Professor Gregory Underhill

Abstract

Cell membrane engineering is an emerging approach in the field of tissue engineering which aims to exploit the modification of cell membranes for a variety of applications including cell homing and retention, stem cell-tethered biosensors, and cell-mediated drug delivery. Compared to procedures requiring genetic manipulation, cell membrane engineering may exhibit several advantages such as decreased cell manipulation, a decreased effect on cell viability and proliferation, and a quicker translation towards *in vivo* studies. In particular, the ability to systematically manipulate the chemistry of cell membranes could form the basis for new investigations into cell functions, including most notably, the analysis of cell-microenvironment interactions. Further, the combination of cell membrane engineering with the optimization of biomaterial scaffold encapsulation techniques could potentially provide unprecedented control of cell-biomaterial interfaces which are critical in defining cellular processes such as stem cell differentiation.

This Thesis describes the development and optimization of methods for the conjugation of biomaterial polymers to the membrane of pluripotent stem cells (mouse embryonic stem cells). Such methods have not previously been reported for embryonic stem cells, and thus, we aimed to establish with this work a foundation for future applications aimed at cell labeling or the defined modulation of cell functions.

In order to perform quantitative analysis of stem cell membrane conjugation procedures we primarily employed a flow cytometry based approach utilizing fluorescently labeled biomaterial components. Specifically, we examined the efficiency of NHS-based biomaterial conjugation, the efficiency of an unexpected acrylate-based conjugation finding, and the combinatorial effects of UV light exposure. In addition, we systematically optimized dosage effects and explored the potential influence of biomaterial conjugation on cell viability as well as the retention of biomaterial domains during stem cell culture. The presented studies demonstrate that embryonic stem cells can be effectively modified on their cell membrane without significantly affecting cell function and expansion. Future experiments building on this work will be focused towards the further elucidation of the functional groups present on the membrane of embryonic stem cells and an improved understanding of the mechanisms underlying membrane conjugation approaches. Overall, these efforts establish a modular method for manipulating stem cells which could serve as an enabling technology for influencing stem cell functions in numerous tissue engineering contexts.

To my parents, for their love and support

ACKNOWLEDGEMENTS

I would first like to thank my adviser, Professor Gregory Underhill, for being a great mentor and allowing me the opportunity to be a member of his lab group to pursue my academic interests. This work represents a long process of support, guidance, and innovation on his part. Despite several setbacks, Dr. Underhill's continual motivation and attention to detail proved invaluable for the project's development. Thank you also for listening and the continual feedback both academically and personally.

I would also like to recognize the entire Underhill Lab group for their encouragement and for teaching me many of the laboratory techniques required for this project. I would especially like to thank Ravi C. Yada for aiding me with the extensive stem cell culture, the lengthy flow cytometry experiments, and in general, for his continual excitement for the project.

I also thank Dr. Barbara Pilas for her support academically and personally. I would also like to thank the Biotechnology Center for access to the flow cytometers.

Most importantly, I would like to thank my parents, Satish and Rama, and my siblings, Rajani and Neal, for their love and support. Thank you for giving me the confidence for completing this process and never losing faith in me.

Lastly, I thank Shamira Sridharan, Shaneen Braswell, and Yanfen Lee for always being there when I needed them, and for their continual encouragement and moral support.

I am also grateful for the funding provided by the National Science Foundation Integrative Graduate Education and Research Traineeship, 'Training the Next Generation of Researchers in Cellular and Molecular Mechanics and BioNanotechnology' (CMMB IGERT, Grant 0965918).

Table of Contents

CHAPTER 1 INTRODUCTION	1
1.1 INTRODUCTION.....	1
1.2 OVERALL GOAL AND SPECIFIC AIMS	3
CHAPTER 2 BACKGROUND.....	4
2.1 THE STEM CELL MICROENVIRONMENT	4
2.2 STEM CELL ENCAPSULATION.....	6
2.3 CELL MEMBRANE ENGINEERING APPLICATIONS.....	10
CHAPTER 3 STEM CELL CULTURE METHODS	13
3.1 INTRODUCTION	13
3.2 CULTURE AND PREPARATION OF MEF FEEDER LAYERS	13
3.3 CULTURE OF MOUSE ES CELLS.....	14
3.3 MEF DEPLETION AND PREPARATION FOR MEMBRANE LABELING	15
CHAPTER 4 NHS-BASED MEMBRANE CONJUGATION OF MOUSE EMBRYONIC STEM CELLS.....	16
4.1 INTRODUCTION	16
4.2 EXPERIMENTAL APPROACH	16
4.3 RESULTS.....	18
4.4 DISCUSSION	20
CHAPTER 5 DOSAGE-DEPENDENT EFFECTS ON LABELING EFFICIENCY	21
5.1 INTRODUCTION	21
5.2 EXPERIMENTAL APPROACH	21
5.3 RESULTS.....	22
5.4 DISCUSSION	24
CHAPTER 6 RETENTION OF BIOMATERIAL LABELING IN SELF-RENEWING ES CULTURE.....	25
6.1 INTRODUCTION	25
6.2 EXPERIMENTAL APPROACH	25
6.3 RESULTS.....	26
6.4 DISCUSSION	29
CHAPTER 7 ACRYLATE-BASED MEMBRANE CONJUGATION & RETENTION	30
7.1 INTRODUCTION	30
7.2 EXPERIMENTAL APPROACH	31
7.3 RESULTS.....	32
7.4 DISCUSSION	37
CHAPTER 8 CONCLUSION AND FUTURE DIRECTIONS	40
REFERENCES	41

Chapter 1 Introduction

1.1 Introduction

Tissue and organ failure is a major health problem within the United States. According to the United Network for Organ Sharing, more than 117,000 Americans are waiting for an organ transplant, but there are only approximately 20,000 organs available each year. To address these concerns, the field of tissue engineering is rapidly becoming a potential alternative, or at least a complementary solution, to transplantation. Researchers are able to implant natural, synthetic, or semisynthetic tissue and organs that are either fully functional from the start or will eventually grow into the required functionality. There are various methods by which to achieve this goal ranging from focusing on using skin equivalents to biomaterials to scaffolds (Nature Biotech, 2000). However, a limitation to these methods can include immunogenicity, rejection, and of course the difficulty of growing specific cell types in large quantities (Koh, 2004). A potential solution to these concerns is the combination of different approaches with stem cells to differentiate stem cells into the desired cell type (**Figure 1**). Along with the ability to differentiate into many specialized cell types, stem cells also maintain the ability to proliferate in an undifferentiated but pluripotent state (Brivanlou, 2003). This makes stem cells an ideal choice for our specific interests.

Elaborating on **Figure 1**, there are currently two main approaches for directing stem cell differentiation: *in vitro* directed differentiation and reprogramming. In the first approach, pluripotent stem cells are generally placed in an *in vitro* environment that is similar to the desired cell type environment. By mimicking both the natural environment and differentiation steps, a specific desired cell type can be produced in an *in vitro* setting prior to implantation back into a human. Some methods to achieve this controlled *in vitro* differentiation include the addition of recombinant growth factors to differentiation media of cells in culture, variations in the intensity of signaling molecules in media, small chemical molecules to enhance, inhibit, or substitute a specific factor in the signaling pathway, formation of embryoid bodies, and finally, the use of co-culture systems. In the latter approach, one fully differentiated cell type can be converted directly into another through the expression of key transcription factors in viral expression constructs. However, there are some challenges to these current approaches.

Some of these challenges include low efficiency in the production of desired cell generation, difficulty in adapting methods used with mouse cells for human cells, and of course, the safety and cost concerns from the reagents used to direct cell fate. For example, reagents used for *in vitro* purposes often contain animal products which can introduce compatibility and immunogenicity concerns if the produced cells are transplanted into humans. Also, even though chemical factors appear to be more beneficial over biological ones, it has been difficult to actually determine their mechanism of action. One specific challenge with the directed differentiation approach is that immature cells with embryonic or early postnatal phenotypes may be produced rather than true adult cells. This may occur due to the fact that cells are in culture for several weeks while cells in the body are developed for a much longer time (Cohen, 2011). The specific challenge with reprogramming is the use of viruses which permanently integrate into the host genome. There are some alternative methods being developed to address these concerns, but they are not as efficient as the viral vector method. Despite being a highly beneficial idea for regenerative medicine with promising results, more work must be completed to determine a more compatible, price efficient, and reliable method for stem cell differentiation.

An emerging solution within the tissue engineering field is that of cell membrane engineering (CME). CME refers to the modification of a cell membrane through biological, chemical, or physical methods to alter cellular functions. Engineering cells to present natural or synthetic ligands on their membrane has becoming a promising way to control and understand cell-microenvironment interactions, cell-cell events, cellular adhesion, and signal transduction (Cheng, 2013; Mahal, 1997). Some examples of CME include cell-mediated drug delivery, cell homing and retention, and stem cell-tethered biosensors. However, most of these stem cell approaches have been studied mainly with mesenchymal stem cells (MSCs) or hematopoietic stem cells (HSCs). There has been little exploration in CME with utilizing pluripotent stem cells for different applications, specifically for understanding or directing differentiation. This idea prompts further exploration to potentially develop a new method that does not require manipulation of the cell from the inside for directing stem cell differentiation, thereby addressing some of the previous concerns. In this Thesis, we investigate several approaches for introducing defined biomaterial components to the cell membrane of pluripotent stem cells.

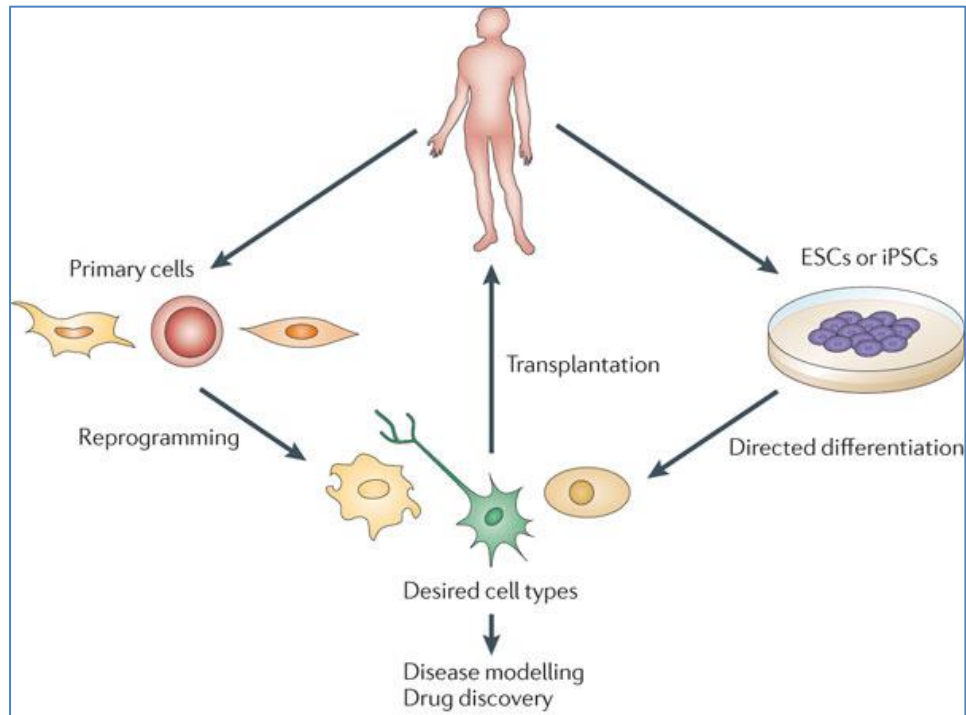


Figure 1: Schematic showing the two current approaches (reprogramming and directed differentiation) to differentiate stem cells to the desired cell types for transplantation back into humans in tissue engineering/regenerative medicine (Cohen, 2011)

1.2 Overall Goal and Specific Aims

Our overall goal in this work was to develop an approach for introducing defined biomaterial moieties to the cell surface membrane of stem cells. These efforts would enable the modulation of cell-biomaterial interfaces and ultimately could be applied towards the analysis and optimization of microenvironmental interactions that regulate directed differentiation/reprogramming. Two specific steps towards accomplishing this overall goal will be further discussed in this Thesis. In Specific Aim 1, we investigated the capability of introducing synthetic biomaterial functional groups, specifically NHS-based biomaterials, to the surface membrane of embryonic stem (ES) cells. In these experiments, we examined the effects of biomaterial linker concentration on cell labeling efficiency, cell viability, and retention in self-renewing culture. In addition, in Specific Aim 2, we systematically explored an unexpected finding of these studies in which acrylate-based biomaterials exhibited cell surface conjugation capability which could be partially modulated by UV light exposure. Collectively, these studies described here provide the foundation for future efforts aimed at the deconstructing cell surface conjugation mechanisms and exploiting these methods for novel applications in tissue engineering.

Chapter 2 Background

2.1 The Stem Cell Microenvironment

Stem cell responses, such as their ability to differentiate and self-renew, depend on the cell's microenvironment, or niche. The niche is important as it maintains stem cells in quiescence and a low metabolic state to prevent stem cell exhaustion. The niche also protects stem cells from accumulating gene mutations (Gattazo, 2014). The microenvironment is composed of various chemical and physical signals that interlink to regulate the fundamental stem cell processes. These signals are generally a result of different soluble factors, such as growth factors or hormones, or insoluble factors, such as cell-cell interactions, cell-extracellular matrix interactions, or surface-bound signaling molecules (Underhill, 2012). Physical forces exerted on the cell or even the shape of a cell could also modulate the signals in various ways. Intrinsic genetic pathways then regulate these extrinsic signals and determine the cell's response to a specific signal. Aside from self-renewal and differentiation, some of the other fundamental processes include: apoptosis, migration, or biosynthesis/metabolism (Zhang, 2008; Metallo, 2007). The inputs from the microenvironment and its consequent effects can be seen in **Figure 2**.

The major component of a stem cell's microenvironment is the extracellular matrix (ECM). The ECM is able to either directly or indirectly regulate the cell behavior and plays essential roles during development. ECM's physical properties such as rigidity, porosity, topography, and insolubility effect cell division, tissue polarity, and cell migration (Gattazo, 2014). These physical properties play a significant role in engineered microenvironments. The ECM's biochemical properties, specifically ECM stiffness, also influences cell behavior since cells sense these external forces and respond accordingly. Cell-ECM interactions can be mediated by cell receptors, such as integrins, and play a significant role in the adhesion, anchorage, and homing of stem cells. To investigate the specific functions of different ECM components in stem cell niches, *in vivo* studies are ideal. However, the niche is so complex and there are many different factors which play simultaneous roles, that these studies become very complex and difficult.

One way to address the previous challenge and understand the effect of the microenvironment on cellular responses is through *in vitro* engineered microenvironments. Engineered microenvironments have been increasingly successful in controlling stem cell fate by mimicking the key regulatory signals from native stem cell microenvironments. The different engineered microenvironment methods include micropatterning, high-throughput arrays, bioreactors/microfluidics, and computational models (Metallo, 2007). The specific engineered microenvironment that we are interested in exploring further is the culturing of cells in confined areas, such as in alginate or agarose beads or even three-dimensional (3D) polymer scaffolds or hydrogels.

Elaborating on some of the different approaches, micropatterning can be used to control specific cell positioning, shape, and exposure to ECM proteins in two dimensional (2D) cultures. The ECM proteins are patterned on a surface with a micrometer resolution. This technique has been used prominently to investigate the influence of cell shape and cell-ECM interactions. In another method, PDMS stamps can be used to mold microwells using hydrogels composed of agarose, polyacrylamide, or poly(ethylene glycol) (PEG). These microwells are typically used for high-throughput analysis to better understand cell-cell interactions. Combining both the microwell and micropatterning approaches, researchers have also been able to form ES cell aggregates with tightly controlled diameters to understand the role of cell-cell interactions in ES cell differentiation. To also examine ES cell differentiation, PDMS can be molded into an array of vertical posts over which cells can be cultured. Depending on the height of these vertical posts, the substrate rigidity will be different, thus providing a different environment for the stem cells. For example, short vertical posts have a stiff environment while a taller vertical post will mimic a soft environment. These micropillars also allow for a greater understanding of ES cell differentiation in respect to traction force, focal adhesions, and cytoskeletal tension. Another high-throughput analysis makes use of cellular microarrays. The microarrays consist of either printed spots of biomolecules with cells seeded on top or direct live cells encapsulated in hydrogel droplets to study the role of combinations of different ECM proteins in cell processes. Again, providing another technique to understand how differentiation is regulated by combinatorial signals (Underhill, 2012). This can also be understood computationally using statistical methods and network models.

To understand the effects of the mechanical properties from the microenvironment on stem cells, hydrogels can also be chemically modified to present either native ECM proteins or adhesive peptides. Hydrogels, especially PEG-based systems, can be tuned based on porosity and mechanical properties. They can also be co-encapsulated or conjugated with bioactive factors to add biological functionality in a controlled manner. I will further discuss hydrogels specifically for stem cell encapsulation methods, in the following section.

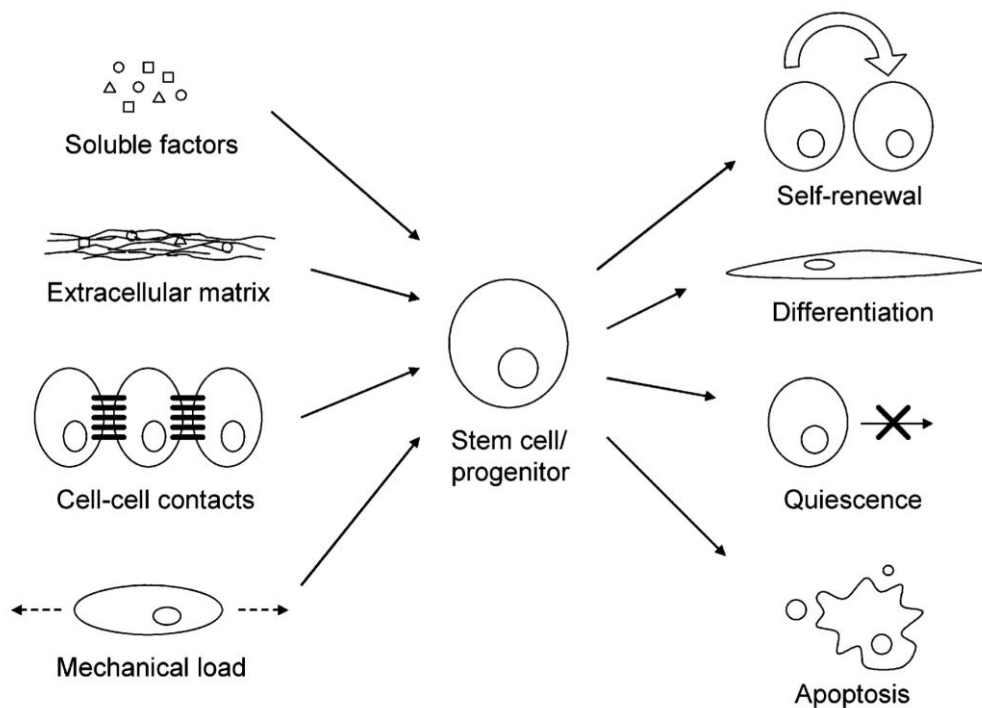


Figure 2: Schematic displaying the various cellular responses resulting from different microenvironmental inputs (Metallo, 2007)

2.2 Stem Cell Encapsulation

As previously mentioned, hydrogels are one type of encapsulation method to mimic a cell's microenvironment. The most common type of hydrogel used for these studies are PEG hydrogels. PEG hydrogels can act as matrices for the controlled release of biomolecules or even as scaffolds for regenerative medicine. The primary advantage of using hydrogels is that not only can they simultaneously encapsulate cells and various biomolecules and are biocompatible, but they also allow one to control the release of

biomaterials through systematic changes in the gel's physical and chemical structure (Lin, 2008).

PEG hydrogels can be formed by various methods of gelation, such as by physical, ionic, or covalent interactions, but it is the different chemical or covalent-crosslinking leads that form the stable hydrogel structures. This in turn allows for tunable physicochemical properties, such as permeability, molecular diffusivity, equilibrium water content, elasticity, and degradation rate. When degradable linkers are introduced to the covalent crosslinks, it allows for the fabrication of well-defined network structures with adaptable properties in time. For our particular purpose, the synthesis of covalently crosslinked PEG gel networks is caused by a chain-growth crosslinking reaction mechanism (**Figure 3a**). These networks are generally formed from functional PEG molecules, such as PEG-di(meth)acrylate (**Figure 3b**), which is what we want to accomplish in Aim 2. Polymerization is caused by free radicals generated from redox reactions or from the photocleavage of initiator molecules. The propagation of these radicals through multiple carbon-carbon double bonds on PEG monomers results in covalently crosslinked chains. The advantage of using a photopolymerization method to form stable hydrogels is that this process takes simply a few minutes. This reduces exposure of biomaterials to thermal energy which in turn reduces negative effects on proteins and cells drastically (Lin, 2008).

Hydrogels can also serve as an ideal model for studying controlled stem cell differentiation. Since, as previously mentioned, stem cells are naturally surrounded by a matrix that provides biochemical signals and a structure for physical cell-matrix interactions to occur (Vincent, 2013). A hydrogel, or even a hydrogel-like system, can mimic this type of environment. There are different ways to achieve this differentiation. One can incorporate bioactive molecules with PEG-based hydrogels or one can even retain cell-secreted biomolecules with the hydrogels. The benefits of the latter are that it can be utilized only when needed, such as during differentiation processes, and their bioactivity could have a greater effect than synthetic analogs which are covalently incorporated within the gel environment (Lin, 2008). As shown with alginate hydrogels, stem cell differentiation was found to be either directly influenced by the cell's ability to deform rigid substrates or indirectly affected by the cells first degrading the matrix and then contracting it. As can be seen in **Figure 3c**, the chemistry and mechanics of cell-

biomaterial interactions can also significantly influence stem cell differentiation. The chemical conjugation of polymer chains to stem cell membranes could potentially play an important role. For our overall goal, we aim to find an intermediate solution and develop an approach for modulating cell-biomaterial interactions within 3D hydrogel scaffolds.

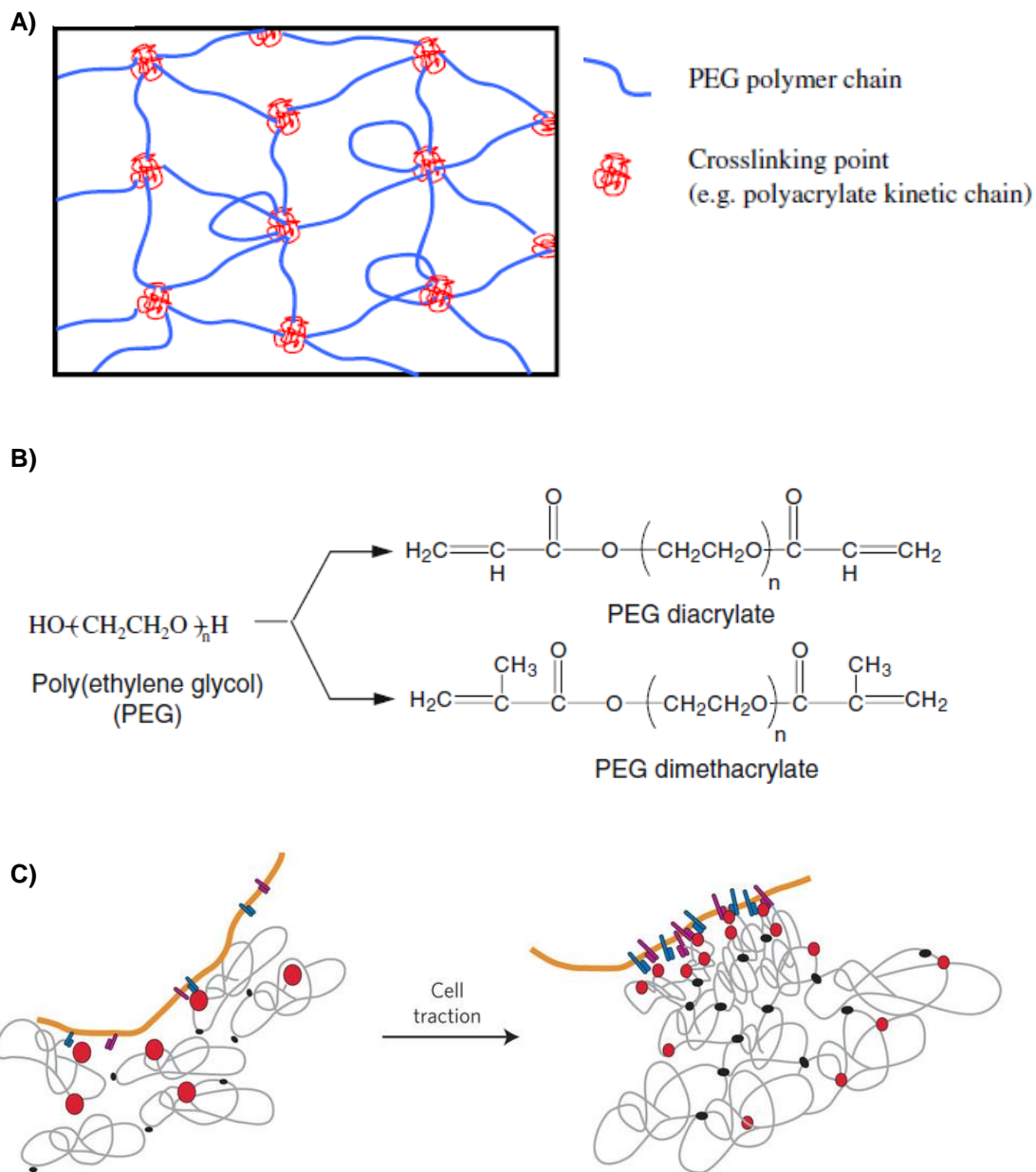


Figure 3: Schematic displaying a) PEG hydrogels formed by the chain-growth method b) the chemical structure of PEG and di(meth)acrylate derivatives that form the hydrogel networks for cell encapsulation (Lin, 2008) and c) how cell traction forces can affect the clustering of polymer chains to membranes in hydrogels which in turn effects stem cell differentiation (Vincent, 2008)

2.3 Cell Membrane Engineering Applications

CME controls different cell-microenvironment interactions that regulate many biological events and play a critical role in tissue regeneration. There are many applications for stem cell membrane engineering resulting from microenvironmental interactions, some examples of which can be seen in **Figure 4**.

One such example includes cell homing and retention, which is the navigation of cells, such as stem cells, to targeted tissues, for example, injured tissues. Human bone marrow-derived mesenchymal stem cells (hMSCs) target receptors are expressed on inflamed vessels of injured tissues. Specifically, inflammatory cytokine-activated endothelial cells express adhesion molecules that induce the rolling of leukocytes and recruit them to the inflamed tissues. The endothelial cells also express vascular cell adhesion molecules which allow for firm adhesion of leukocytes. In the paper by Cheng *et al.*, the research team modified the membrane surfaces of the hMSCs to conjugate synthetic ligands (E-selectin targeting peptides) to control the binding of stem cells on adhesion molecules. By modifying the kinetics of the interaction between peptides and selectins, they were able to engineer hMSCs to firmly adhere or roll under physiologically relevant shear stresses. For example, in one of their tests, they found that stem cells modified with peptides that strongly bind to selectins remain bound under physiological flow and do not roll, while peptides that bind to selectins with fast dissociation rate constant roll in the direction of flow. Overall, they found that their approach did not affect cell viability, proliferation, or multipotency, but it did open the doors for cell homing and retention in other diseases/instances (Cheng, 2012).

Another example for a CME application is the modification of stem cell membranes to tether biosensors to better understand cell signaling and cell-to-cell communication, especially in real time. This allows for a greater understanding and tracking of transplanted cells; once again of cell homing to sites of inflammation. Specially, Zhao *et al* covalently attached fluorescent nucleic acid aptamer sensors with surface anchoring moieties to the surface of cells to produce a real-time signal when target molecules (platelet-derived growth factors [PDGF]) contact the cell surface (MSCs). Upon contact, the PDGF sensor brings two attached dyes within close proximity and a fluorescence signal is produced which is then detected in real time. By using this simple method of

CME, there is no need for complex genetic engineering approaches and this application already has potential for *in vivo* applications. This method is also significant because it allows for the understanding of cellular response to cues in the microenvironment in both time and space (Zhao, 2011).

The final example I will discuss is that of cell-mediated drug delivery by CME methods. In this application, adjuvant drug-loaded nanoparticles are conjugated to the surfaces of HSCs and T cells. In Stephan *et al*, this was done so by cell-surface thiols. In general, cell-mediated delivery allows for maximum donor cell efficacy and *in vivo* persistence, the offset of suppressive molecules at cell homing sites, and the promotion of differentiation of transferred cells into a therapeutically optimal phenotype. Using this particular method, Stephan *et al* showed that adjuvant agent-releasing particles can be stably conjugated to cells without toxicity or interference with intrinsic cell functions, mimic *in vivo* migration patterns of the carrier cell, and the carrier cell has enhanced function using low drug doses that typically have no effect when given by traditional systemic routes (Stephan, 2010).

As was mentioned, CME methods are less complex than current procedures, such as genetic engineering or cancer immunotherapy. For example, with cancer immunotherapy methods, adjuvant drugs are necessary to maximize and maintain high levels of therapeutic cell efficacy. With genetic engineering, there are regulatory and cost barriers related to large-scale production, costly and lengthy protocols, technical challenges, and necessary small-molecule drugs that cannot be genetically encoded (Stephan, 2010). CME provides an alternative to these current approaches and addresses many of previously stated concerns while making CME a step closer to *in vivo* procedures. This makes cell membrane engineering a desirable approach and the one which we chose to combine with our embryonic stem cells to modulate cell-biomaterial interactions for differentiation.

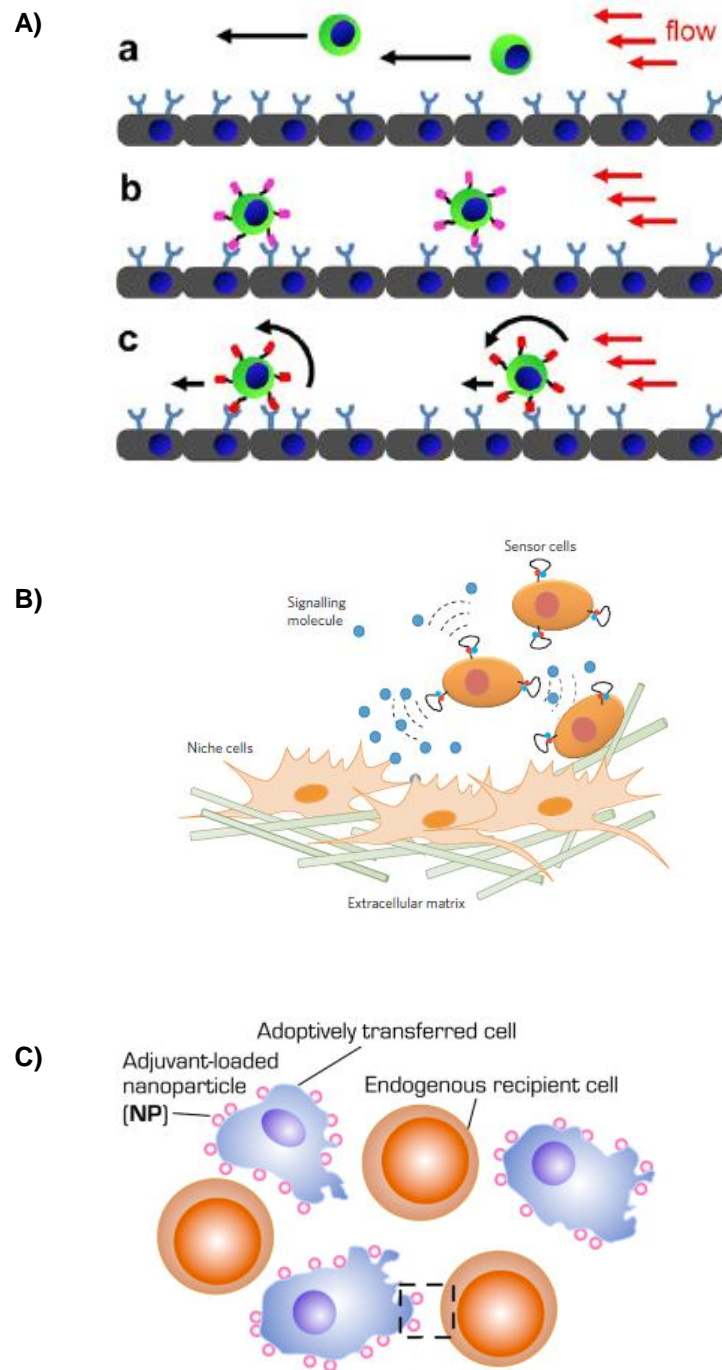


Figure 4: Three different cell membrane engineering applications: a) human mesenchymal stem cell recruitment to injured tissues (Cheng, 2012), b) covalent attachment of fluorescent nucleic acid aptamer sensors with surface anchoring moieties to mesenchymal stems cells thus creating a stem cell biosensor (Zhao, 2011), and c) drug-loaded nanoparticles conjugated to human stem cell membranes for cell-mediated drug delivery (Stephan, 2010)

Chapter 3 Stem Cell Culture Methods

3.1 Introduction

To investigate cell-biomaterial modular linkages to cell membrane surfaces, we utilize embryonic stem cells. This chapter provides a general methodology for the culture and preparation of embryonic stem cells for growth and membrane labeling. Specific culturing and final preparation methods for individual experiments will be discussed in further detail in the appropriate chapters.

3.2 Culture and Preparation of MEF Feeder Layers

The first step in this process is the expansion of the Mouse Embryonic Fibroblasts (MEFs). MEFs serve as a feeder layer for mouse embryonic stem cells (mESCs) thereby providing the cells with the nutrients they need for survival. MEFs also can provide factors that enhance the proliferation and maintain the undifferentiated states of embryonic stem cells (Xu, 2005).

To expand MEF cells, first, six T150 culture flasks are coated with 7mL of 0.1% gelatin (dissolved in distilled water) and placed in an incubator (37°C and 5% CO₂) for 15-20 minutes. During this time, 5×10^6 MEF cells (*PMEF*, *Strain CF-1*, *Untreated*, *EMD Millipore*) are thawed and resuspended in 12mL of MEF media. MEF media components include: 87.5% DMEM, 10% Fetal Bovin Serum (FBS), 0.5% Penicillin/Streptomycin, 1% L-glutamine, and 1% Minimum Essential Medium Non-Essential Amino Acid (MEM NEAA). At the end of the time period, the gelatin is aspirated from the culture flasks and the flasks are washed once with 1X Phosphate Buffer Solution (PBS). To each flask, 23mL of MEF media and 2mL of the MEF cell suspension is added and then the flasks are placed back in the incubator to for MEF cells expansion. After about 1-2 days, the old media is aspirated and the fresh MEF media is added (25mL). At this stage, the MEF cells are generally ~35-40% confluent. 1-2 days after this point, MEFs are usually ~80-90% confluent. This means that there is generally a single layer of growing MEF cells, with some overlap, coating most of the gelatin layer and the cells need to be growth arrested.

For the growth arrest process, Mitomycin C (*Sigma-Aldrich*) is used. Mitomycin C inhibits DNA synthesis by forming crosslinks between complementary strands of DNA so that the strands cannot separate. This in effect inhibits DNA replication and prevents the

MEF cells from growing (Verweij, 1990). In our case, the light-sensitive Mitomycin C powder (2mg) is first reconstituted with 1X PBS (4mL) to obtain a working stock concentration of 0.5mg/mL and then sterilized with a syringe filter. The sterile Mitomycin C is further diluted to 10µg/mL with MEF media. The old culture media from the flasks is aspirated and 16.8mL of the Mitomycin C MEF media solution is added to each flask. The flasks are then placed back into the incubator for another ~3 hours. At the end of this time, the Mitomycin C MEF media solution is removed and the culture flask rinsed with sterile 1X PBS. 0.25% Trypsin is added to each culture flask and the cells are again placed back in the incubator for 5 min. As in regular cell culture, MEF media is added to stop the trypsin and the suspension is centrifuged (5 minutes at 1000 RPM). The supernatant is aspirated and the MEFs resuspended in ~10mL of MEF media. The cells are then counted and aliquoted (the cells were centrifuged after counting and appropriate volume of MEF freeze media (77.8% MEF media, 12.2% FBS, and 10% DMSO) added) so that there are approximately 1 million cells per cryovial (for a total of ~7 cryovials). The cryovials are transferred to a freeze container and placed in the -80°C fridge for ~24 hours. After about a day, the cryovials are transferred to a liquid Nitrogen tank.

3.3 Culture of Mouse ES cells

Similar to the MEF culture, gelatin (5mL) is added to two 10cm petri dishes and incubated for 15-20 minutes. During this time, a frozen vial of MEF cells are thawed in 19mL of MEF media and centrifuged (for each petri dish). The supernatants are aspirated and the cells suspended in 10mL of MEF media each. At the end of the 15-20 minutes, the gelatin layers are aspirated, washed, and the MEF cell suspensions are added. The petri dishes are both placed back in the incubator to allow the MEF cells to grow overnight.

After about 24 hours, the MEF cells are generally ~95% confluent, with some cells overlapping. At this point, thaw a frozen vial of mESC and add it to ES growth media (82.3% DMEM, 15% ES-qualified FBS, 0.5% Penicillin/Streptomycin, 1% L-glutamine, 1% MEM-NEAA, and 2mL of 2-mercaptoethanol in PBS from a stock solution of 50mM). Centrifuge this solution and aspirate the supernatant. The ES cells are resuspended in 12mL of ES growth media with 12µL of Leukemia inhibitory factor (LIF, *Millipore*). LIF maintains mESCs in an undifferentiated state so it is important to add fresh LIF every

22-24 hours. Aspirate the MEF media from the MEF cells and rinse with sterile 1X PBS. After the PBS has been removed, add in the ES cell suspension to the MEF layer and incubate for ~22 hours.

One day (~22 hours) after the ES cells have been plated, the confluency of the cells is normally ~5%. Again, the old media is aspirated and a fresh solution of ES media + LIF is added to the cells. After ~20 hours, the ES cells are generally ~25% confluent and the media is changed once again. By the third day, mESCs are generally ~75-80% confluent. It is at this point when mESCs are either typically frozen down or used for experiments. mESCs can also be passaged with no greater than 1/8 dilution on a new MEF feeder layer.

3.4 MEF Depletion and Preparation for Membrane Labeling

Once the mESCs reach ~75-80% confluency, they undergo a MEF depletion to isolate the mESCs from the MEF cells as this will ensure an accurate mESC cell number for the next step. For this depletion, the old media is aspirated from the mESCs, trypsin (6mL) added, and the cells are incubated. After 5 minutes, ES media is added to counteract the trypsin. The cells are centrifuged and the supernatant aspirated. The mESCs are then resuspended in 15mL of ES media and counted. If the cells will be frozen down, then freeze media (90% ES media and 10% DMSO) is added to the cell suspension and 1×10^6 cells + freeze media are added per cryovial (typically ~10 cryovials). The cryovials are transferred to a freeze container and placed in the -80°C fridge for ~24 hours. After about a day, the cryovials are transferred to a liquid Nitrogen tank. In terms of experiments, usually 4.7×10^6 mESCs are added to 9.4mL of ES media, but generally, the desired concentration is 0.5×10^6 cells/1mL ES media. It is at this concentration that the cells may be further divided for the appropriate experimental conditions and/or biomaterial added. However, as previously mentioned, the detailed membrane labeling methodology will be outlined in the applicable *Experiment* sections for the following chapters.

Chapter 4 NHS-Based Membrane Conjugation of Mouse Embryonic Stem Cells

4.1 Introduction

As mentioned in Chapter 1, we aim to develop an approach for modulating cell-biomaterial linkages so that we can effectively guide their interactions with the microenvironment and thus direct stem cell differentiation. However, first, we must perform initial studies to better understand biomaterial attachment to cell membrane surfaces. It is essential to optimize the biomaterial concentration added to the stem cell surfaces that will be detectable on a single day, and ideally over the course of multiple days. This initial detection will introduce the possibility of a new CME method.

4.2 Experimental Approach

Initially, we tested a NHS-based biomaterial (NHS-PEG-Biotin, or NPB for short) on the surface of mouse embryonic stem cells (mESC). This system was chosen because 1) NHS is known to form an amide bond with amines that are located on cell membrane surfaces and 2) biotin allows us to obtain a fluorescent readout based on biotin and fluorescent streptavidin chemistry (Biotin-Streptavidin Alexa Fluor 647 (SAF647) or Biotin-Streptavidin Alexa Fluor 488 (SAF488)). The actual fluorescent readout is obtained either quantitatively (flow cytometry (BD LSR)) or qualitatively (fluorescent microscope (Olympus IX81 Inverted Cell Culture Microscope)). The process used to label the biomaterial on the mESC surface can be seen in **Figure 5**.

As mentioned above, one of techniques utilized to detect the conjugation of a biomaterial on the cell surface is flow cytometry. Flow cytometry measures the properties of single particles when they are in suspension. While in a tube, the particles are randomly scattered in 3D space, but a flow cytometer contains a fluidic system which allows a single file of particles to flow through the system. Specifically, the sample is injected into a central channel that is enclosed by an outer sheath containing faster flowing fluid. As the sheath fluid moves, it creates a drag effect on the narrowing central chamber which in turn alters the velocity of the central fluid so that the flow front becomes parabolic. This as a result creates the single file of particles. These particles then cross through a beam of lights and the light is scattered. Light that is scattered in the forward direction (FSC) provides information about the particle's size and generally is used to determine the difference between debris and living cells. The side scatter channel (SSC) provides

information on the granularity of a particle. To analyze the flow cytometry data collected, “gating” is used to eliminate unwanted particles. For example, dead cells and debris usually have a lower FSC than living cells, so the gate will be drawn around higher FSC values indicating alive cells, thus removing the dead cells from the system to be analyzed. These gates are drawn until the population of interest is determined and a histogram is produced based on this analysis (Rahman, 2009).

For this specific set of experiments, 7.2 mg of NPB (MW 3400 Daltons) powder is dissolved in 250 μ L of DMSO to obtain an initial concentration of 420 μ M. This concentration is then added to 2.35×10^6 MEF depleted mESCs for 10 minutes at room temperature. NPB remaining in solution, consequently not conjugated to a cell membrane surface, is washed out of the system using PBS. As a control, 2.35×10^6 cells are also treated with 250 μ L of DMSO only. The mESCs in both conditions are resuspended in 2.35mL of ES Media and 2.35 μ L of LIF prior to splitting the cell suspension. 1mL (1×10^6 cells) of the cell suspension is used for Day 0 studies while 800 μ L (800,000 cells) of the suspension is plated in a second well plate for next day (Day 1) studies.

For the imaging based approach, SAF488 is added to 1×10^6 cells for 10 minutes at room temperature in the dark. To remove unconjugated SAF488, the system is first rinsed with FACs buffer (PBS + 2% BSA) and then the fluorescently labeled cells are resuspended in 1mL of FACs buffer. This solution is then transferred to well plates before imaging.

Similarly, for flow cytometry, SAF647 is added to 1×10^6 cells for 10 minutes at room temperature in the dark. Again, the system is washed with FACs buffer to remove unconjugated SAF647 and the cells resuspended in 1mL of FACs buffer. The cells are kept in suspension in a tube.

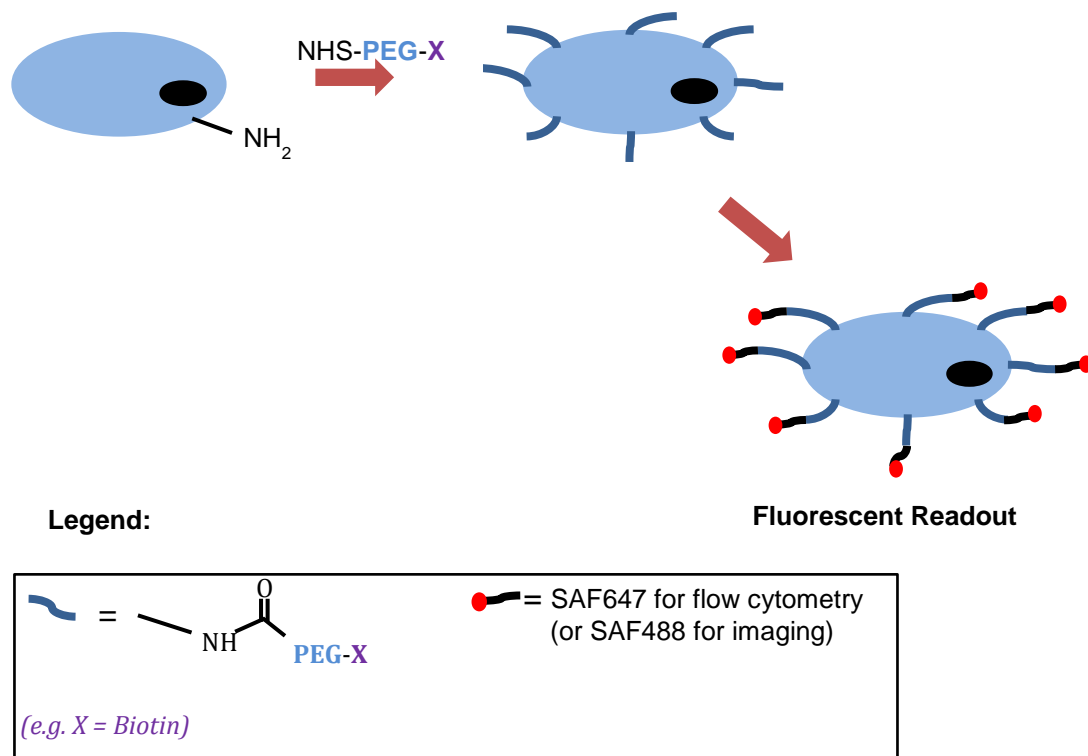


Figure 5: NHS-based biomaterial conjugation to amines located on a mouse embryonic stem cell membrane. Using well known biotin-streptavidin chemistry, a fluorescent streptavidin is bound to the NHS-based biomaterial. The resulting fluorescence is captured by either flow cytometry or imaging methods.

4.3 Results

During flow cytometry, data is collected for 10,000 alive cells in a FSC-A vs SSC-A gate. The desired cell population is further obtained from gating the new cell population obtained from the first gating. The second gate is based on FSC-W vs FSC-A plot. The resulting histogram can be seen in **Figure 6a**.

Theoretically, mESCs treated with NPB should bind to cell surface amines through amide bonds between the cell membrane amine group and the biomaterial NHS group. This idea is confirmed, as there is a noticeable shift in fluorescence when NPB (420 μ M) is added to the system compared to mESCs that did not receive this biomaterial dosage. However, there appears to be two peaks in the treated mESC histogram indicating heterogeneity in labeling and detection. During microscopy, there again is

noticeable fluorescence detection when NPB is introduced in the system (**Figure 6b**). Thus once again confirming the conjugation of NPB to mESC cell membranes. However, it is difficult to see the heterogeneity with fluorescent microscopy despite it being clearly shown with flow cytometry. At this specific concentration, there are no imaging or flow cytometry multiple day data. Prior to imaging on Day 1, majority of the mESCs were floating in the media solution rather than attaching once again to the MEF layer.

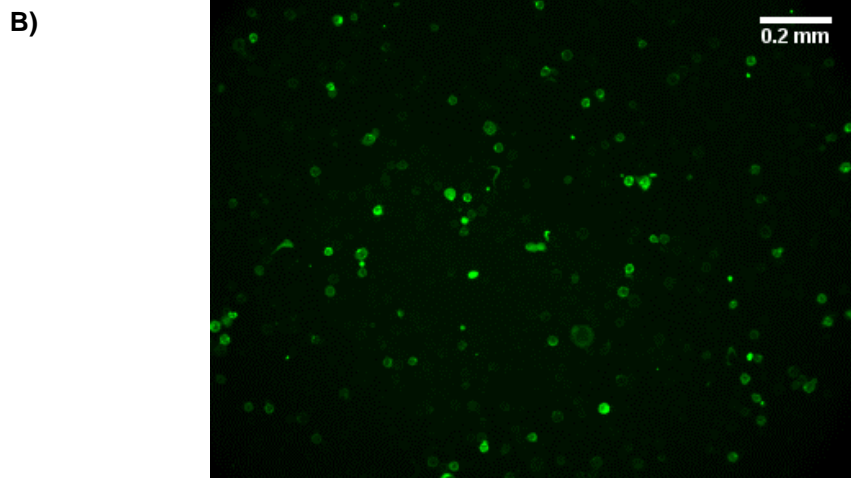
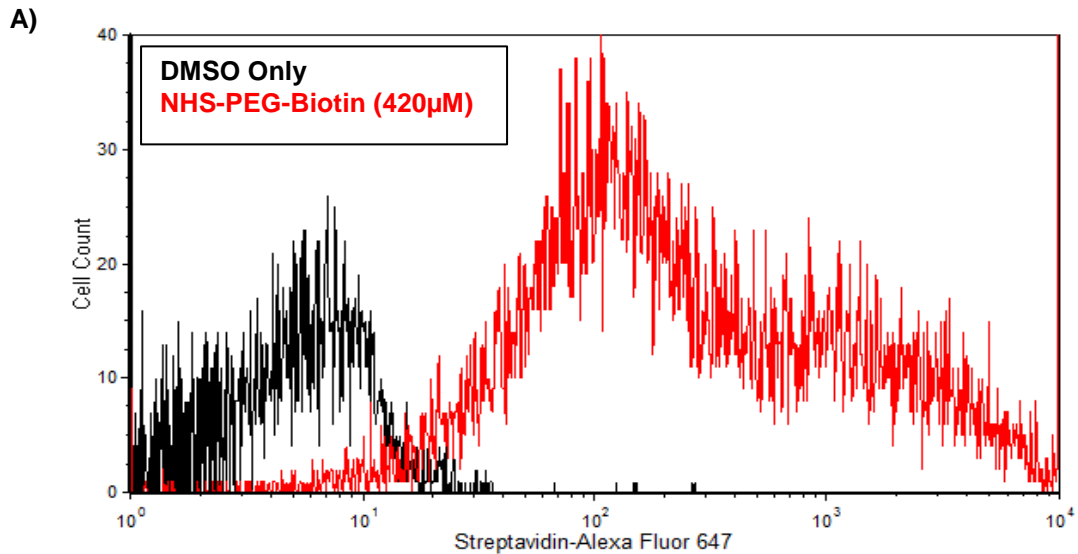


Figure 6: NHS-PEG-Biotin (420µM) conjugated on mESC (1×10^6 cells) cell membranes has detectable fluorescence on Day 0 using both a) flow cytometry methods and b) fluorescent microscopy

4.4 Discussion

This inhibition of cell adhesion to the feeder layer and subsequent inhibition of cell proliferation indicates a cell “pegylation”. The concentration of NPB is possibly so high that the PEG components of the linker on the mESC surface may be very close to one another and encapsulate the cell. This could also potentially mean that the components of the cell membrane surface which normally attach to the MEF layer are now blocked by the PEG components of the biomaterial linker. Thus, indicating a need to lower and optimize the NPB concentration added.

Chapter 5 Dosage-Dependent Effects on Labeling Efficiency

5.1 Introduction

As seen in the last section, NPB at 420 μ M does have a strong and detectable fluorescent signal, but it causes the cells to be “pegylated”. This cell pegylation negatively impacts cell viability over time, as the cells are not able to reattach to the MEF layer. To address this “pegylation” concern, we performed a dose-dependent response experiment to optimize the concentration of biomaterial added to the surface. We do this because a high concentration may alter biological functions of the cells and pegylation may occur again, while a low concentration may not make the necessary modifications for the desired impact. We chose to investigate four other concentrations using a serial dilution method to determine which concentration(s) would give us a detectable fluorescence on a single day. Our hypothesis, based on the previous initial conjugation, is that as the concentration of the biomaterial linker decreases, there should be fewer linkers conjugating to the mESC surface membranes, **Figure 7**, thus correlating to a decrease in fluorescence.

5.2 Experimental Approach

The process used to label the biomaterial on the mESC surface is similar to that of the schematic in **Figure 5**. For this specific set of experiments, 7.2 mg of NPB (MW 3400 Daltons) powder is again dissolved in 250 μ L DMSO to obtain an initial concentration of 420 μ M. Through serial dilutions, the following concentrations are obtained: 210 μ M, 105 μ M, 52.5 μ M, and 26.3 μ M. Each concentration is added to 2.35×10^6 MEF depleted mESCs for 10 minutes at room temperature. NPB remaining in solution is washed out of the system using PBS. As a control, 2.35×10^6 cells are also treated with 250 μ L DMSO. The mESCs are resuspended in 2.35mL of ES Media and 2.35 μ L of LIF. 1mL (1×10^6 cells) of cell suspension is pulled out for Day 0 studies.

For the imaging based approach, SAF488 is added to 1×10^6 biomaterial labeled and control cells for 10 minutes at room temperature in the dark. To remove unconjugated SAF488, the system is rinsed with FACs buffer. The mESCs are resuspended in 1mL of FACs buffer and the solution transferred to well plates prior to imaging.

Similarly for flow cytometry, 10 μ L of SAF647 is added to both biomaterial labeled and control cells (1×10^6 cells each) for 10 minutes at room temperature in the dark. To remove unconjugated SAF647, the system is rinsed with FACs buffer. The mESCs (1×10^6) for each condition are then resuspended in 1mL of FACs buffer and used for flow cytometry.

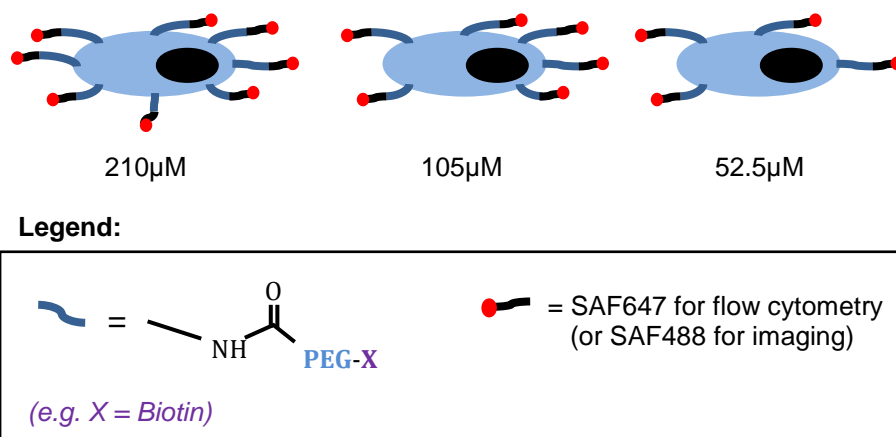


Figure 7: A schematic displaying a decrease in dosage of biomaterial (NPB) added may correlate to a decrease of biomaterial conjugation to the mESC surface membrane

5.3 Results

During flow cytometry, data is collected for 10,000 alive cells in a FSC-A vs SSC-A gate. The desired cell population is further obtained from gating the new cell population obtained from the first gating. The second gate is based on FSC-W vs FSC-A plot. The cell population from the second gating is used to draw the histograms in **Figure 8**.

As can be seen in the flow cytometry histograms in **Figure 8**, the four concentrations are shifted towards the right when compared to the DMSO only control, indicating both a detectable and high level of fluorescence. It is also seen that as the dosage of the NHS-based biomaterial linker added decreases, so does the level of fluorescence. This shows that there may in fact be fewer biomaterial linkers conjugating to the cell surface as the concentration of linker added to the system decreases, all conditions contain the same number of cells, as initially predicted.

With imaging, higher levels of fluorescence are seen as the mESCs are treated with the NPB compared to the mESCs which simply have DMSO added to them. For example in

Figure 9, in the DMSO only image, there is some background noise, but in the image with the mESCs treated with NPB at 105 μ M, there is a significant increase in fluorescence levels.

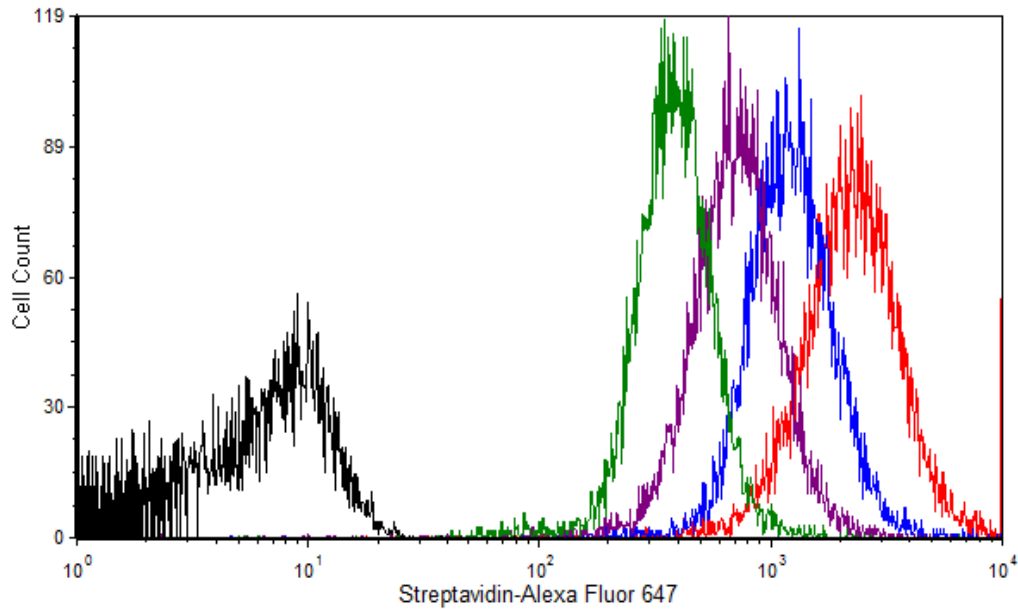


Figure 8: Using flow cytometry, there is a noticeable dosage dependent response. There is a decrease in fluorescence as the dosage of NPB added decreases, thus indicating a decrease in NPB binding to the mESC surface membrane. The four different dosages added are all detectable by flow cytometry on Day 0

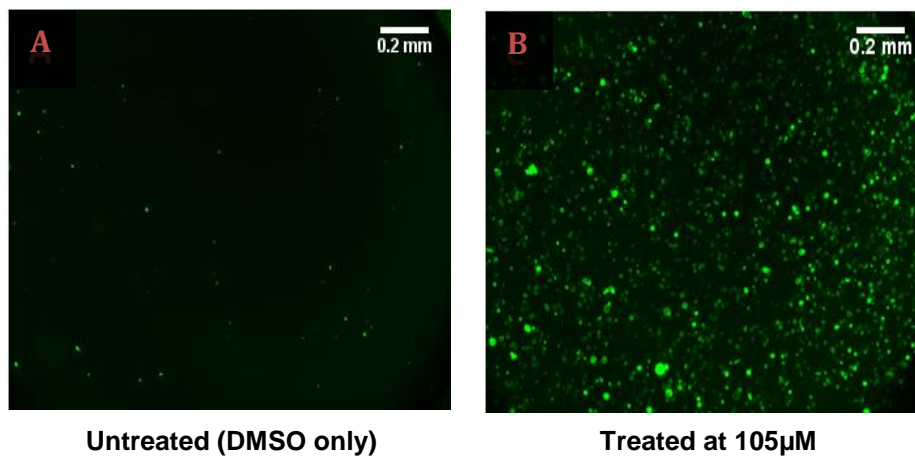


Figure 9: The fluorescence is also detectable by imaging on Day 0. For example, the DMSO only control (no NPB added) shows some background signal, but the mESCs treated with NPB at 105 μ M shows a significant increase in fluorescence levels compared to the control mESCs

5.4 Discussion

With the dosage dependent response experiments (**Figure 8**), it is seen that even at the lowest concentration of biomaterial linker (26.3 μ M), there is still a detectable level of fluorescence, indicating cell surface modifications. The lower dosage does have a lower level of detectable fluorescence when compared to the higher dosage treatments indicating fewer surface modifications comparatively. This in turn correlates to the mESCs being closer to a “natural” state. At these concentrations, specifically for 105 μ M and lower, there is less negative cell viability as there are more alive cells during the gating procedure.

Since it is not possible to determine the exact amount of mESC surface modification with flow cytometry, we use a Biotin Quantitation Kit (*Thermo Scientific*) in combination with a plate reader. Since this is a fairly sensitive assay, we decided to use NPB at 105 μ M since has less negative cell viability but yet a strong and detectable fluorescence level. We determined that 14.7pmol/10 μ L of NHS-based biotin binds to the surface of mESCs.

Now that we have a range of NPB dosages which fit our criteria, with an exact optimal concentration, the new question that arises is how do mESCs treated with 105 μ M behave when they are replated over multiple days.

Chapter 6 Retention of Biomaterial Labeling in Self-Renewing ES Culture

6.1 Introduction

As discussed in Chapter 4, despite NPB at 420 μ M having a strong and detectable fluorescent signal on Day 0, replated mESCs in culture do not reattach to the MEF layer as the cells experience “pegylation”. This cell pegylation negatively impacts cell viability over time. To address the “pegylation” concern, we build upon the previous Chapter’s findings. In this section, we determine how NPB is retained over multiple days, specifically when NPB is added at 52.5 μ M and 105 μ M. These dosages are chosen because they both have a high level of fluorescence detection compared to the control and are at least 4x less than the initial dosage studied which should reduce “pegylation” effects from the beginning considerably. Our hypothesis based on Chapter 4, is that if the mESCs do not experience “pegylation,” the fluorescence should be similar over multiple days with minimal negative effects on the cells.

6.2 Experimental Approach

The process used to label the biomaterial on the mESC surface is similar to that of the schematic in **Figure 5**. 7.2 mg of NPB (MW 3400 Daltons) powder is again dissolved in 250 μ L DMSO to obtain an initial concentration of 420 μ M. Using serial dilutions, NPB concentrations of 105 μ M and 52.5 μ M are attained. These concentrations are added to 2.35×10^6 MEF depleted mESCs for 10 minutes at room temperature. NPB remaining in solution is washed out of the system using PBS. As a control, 2.35×10^6 cells are also treated with 250 μ L DMSO. The mESCs are resuspended in 2.35mL of ES Media and 2.35 μ L of LIF and then divided for three different conditions. 1mL (1×10^6 cells) of cell suspension are used for Day 0 studies, 800 μ L (800,000 cells) are plated in a second well plate for next day (Day 1) studies, and finally, 400 μ L (400,000 cells) are plated in a third well plate for Day 2 studies.

For fluorescent imaging, SAF488 is added to both 1×10^6 biomaterial labeled and control cells for 10 minutes at room temperature in the dark. To remove unconjugated SAF488, the system is rinsed with FACs buffer. The mESCs are resuspended in 1mL of FACs buffer and the solution replated in well plates prior to imaging. For Day 1 experiments, the mESCs are kept on the MEF layer in the well plate and washed with PBS after media removal (ensuring that any unattached cells and debris were out of the

system). SAF488 is introduced and incubated with the cells for 10 minutes in the dark at room temperature. The system is washed with FACs buffer to remove any unconjugated SAF488. 1.5mL of FACs buffer is added to the well plates and the cells are imaged. On Day 2, the cells are not imaged based on the results from Day 1.

Similarly for flow cytometry, 10 μ L of SAF647 is added to 1×10^6 biomaterial labeled and control cells for 10 minutes at room temperature in the dark. To remove unconjugated SAF647, the system is rinsed with FACs buffer. 1mL (1×10^6 cells) of the cell suspension is used for Day 0 studies. On Days 1 and 2, the cells are again trypsinized in the well plates. 10 μ L of SAF647 is added to the cell suspensions for 10 minutes at room temperature in the dark, and again, unconjugated SAF647 is washed from the system using FACs buffer. The mESCS (1×10^6) are resuspended in 1mL of FACs buffer each time and used for flow cytometry.

6.3 Results

During flow cytometry, data is collected for 10,000 alive cells in a FSC-A vs SSC-A gate. The desired cell population is further obtained from gating the new cell population obtained from the first gating. The second gate is based on a FSC-W vs FSC-A plot. The cell population from the second gating is used to draw the histograms in **Figure 10**.

Since we are able to detect fluorescence at Day 0, as seen in the previous Chapter and in the right-most histogram in **Figure 10a**, and there is no significant negative cell viability, the question of whether or not these particular concentrations result in cell “pegylation” arises. From a simple glance at the cells in the well plates on Days 1 and 2, there appear to be more mESC attachment onto the MEF layer and fewer floating cells as the biomaterial dosage decreases. As seen in **Figure 10**, this observation is confirmed with both flow cytometry and imaging methods.

For the multiple day treatments, it is seen that with flow cytometry (**Figure 10a**), the fluorescence reading is detectable for both Days 1 and 2. However, with imaging (**Figure 10b**), a fluorescence signal is not seen as clearly on Day 1, and by Day 2, there is no detectable signal at all. Interestingly, it is seen that there is a clear decrease in the fluorescence level over the course of the three days. Day 0 has the highest fluorescence while by Day 2 the fluorescence level is similar to the untreated control condition. This

decrease is quantified in **Figure 11**, for NPB at 52.5 μ M, where we look at the log average relative fluorescence, based on the geometric mean, for Day 0, Day 1, and Day 2 in respect to Day 0. For Day 1, the average relative fluorescence mean is 1.07 ± 0.01 and for Day 2, it is 1.08 ± 0.002 .

Even though we found a range of dosages that do not appear to display negative cell viability over time and have detectable fluorescence levels, there is a significant unexpected decrease in fluorescence as conjugated mESCs are replated for Day 1 and Day 2 studies. This decrease in fluorescence could potentially be explained by two reasons: 1) the replated mESCs are splitting into daughter cells or 2) due to physical and/or chemical effects.

When mESCs are replated, the biomaterial linkers are possibly dividing amongst daughter cells when the original conjugated parent cell divides. As a result, there are fewer linkers conjugated on a single mESC surface and thus a lowered fluorescence output. In regards to the latter reason, there could be a possibility that the linkers are falling off of the cell over the course of multiple days because the conjugation may not be as strong or the linkers could be recycled during normal cellular processes. Again, indicating fewer linkers conjugating to mESC surface membranes. To investigate this occurrence, we used a CFSE Cell Proliferation Kit (*Life Technologies*) and a drug (STLC).

The CFSE dye labels a cell to trace multiple generations with flow cytometry. It is known to have long-term signal stability and should be non-toxic. By using a similar idea to our previous findings, the fluorescent signal from the CFSE dye should be the highest on the first day. As the days progress, there should be a sequential “halving” of the signal as the parent cells are being split into daughter cells (Matthias, 2011). If this pattern is observed, then it also indicates that the biomaterial linker is being split between daughter cells.

STLC on the other hand, blocks the proliferation cycle and the parent mESC is not able to divide into daughter cells once it has been replated on a MEF layer. When cells on Days 1 and 2 are observed, and the cells have not been dividing, the cells should theoretically retain a similar level of biomaterial conjugation and fluorescence levels as

the cells from Day 0. If there is a slight or even a noticeable decrease in fluorescence, this could possibly indicate that the decrease is due to cell turnover or the biomaterial linker falling off over time.

However, when these experiments were performed (data not shown), high levels of cell toxicity is observed. There is little cell attachment over the multiple days and more dead cells noticed during flow cytometry gating than previously seen.

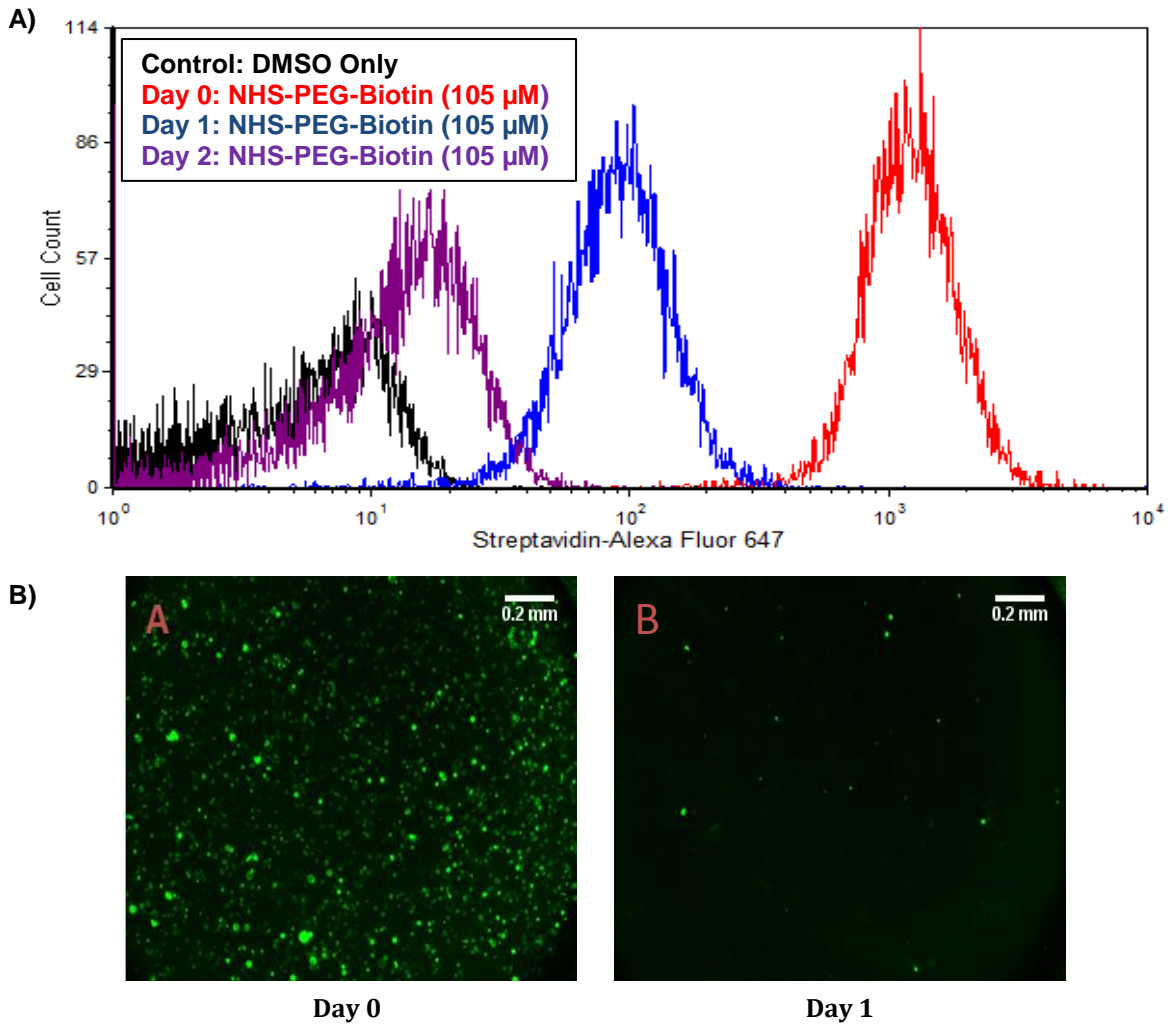


Figure 10: a) There is detectable fluorescence over the course of 3 days, but the fluorescence does decrease each day. By Day 2, the fluorescence for NPB treated mESCs is starting to overlap with the fluorescence histogram for the control mESCs, indicating a decrease in NPB linkers conjugating to cell membrane surfaces. b) There are detectable levels of fluorescence only on Day 0 with imaging. Day 1 images show a fluorescence signal comparable to background fluorescence levels as seen in the DMSO only control. Imaging methods does not appear to be as sensitive of an approach as flow cytometry for our purposes

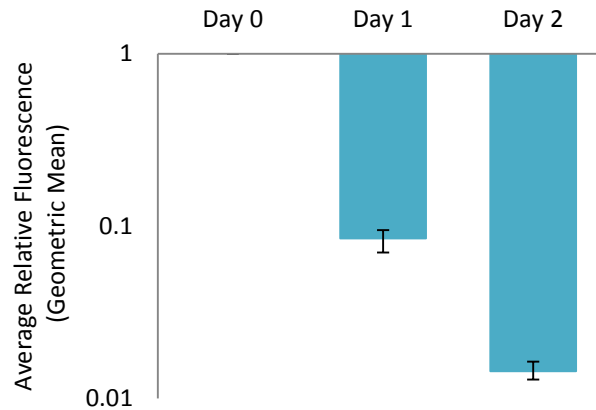


Figure 11: Quantitative analysis showing a decrease in average relative fluorescence over three days when NPB is at 52.5 μ M. This is the same pattern which was seen using flow cytometry for NPB at 105 μ M

6.4 Discussion

Based on the dosage dependent experiments (**Figure 8**), it is seen that NPB dosages at 52.5 μ M and 105 μ M have high detectable levels of fluorescence. In this Chapter, we see that these are in fact optimal dosages to use as there is less negative cell viability and greater mESC reattachment to the MEF layer on Days 1 and 2, thus addressing the pegylation concerns.

We also notice that it is difficult to observe NPB (at 105 μ M) fluorescence on Day 1 with imaging methods, but we are still able to detect fluorescence until Day 2 using flow cytometry. This indicates that imaging is not as sensitive of an assay as is required for these studies and that flow cytometry is the better method to utilize.

Based on both the imaging and flow cytometry results, there is a noticeable decrease in fluorescence over the multiple days. To determine the reason behind the loss of fluorescence in self-renewing mESC culture, we used both CFSE and STLC, but neither method is successful in these experiments. In the future, it is important to analyze either the loss or the partitioning of linkers with an alternative method or through optimization of a different mitotic inhibitor.

Chapter 7 Acrylate-Based Membrane Conjugation & Retention

7.1 Introduction

Based on the previous chapters, we have been able to confirm and optimize NPB conjugation to mESC cell surfaces. There are still some components which require further investigation, but for now, we now shift our attention to the next aim. To reiterate, our goal for the second aim is to explore the capability of modulating cell-biomaterial interactions through the addition of acrylate domains to the cell membrane. The NHS group in the biomaterial linker will bind to the amines on the surface as before, while the acrylate group interacts with another acrylate domain present in the solution via light polymerization, **Figure 12**. Through these interactions, a bond will form between two different biomaterial linkers with one of these linkers already conjugated to the cell surface membrane. This will serve as an initial testing phase prior to investigating cell-cell interactions.

Interestingly, from initial tests, we found that Acrylate-PEG-Biotin (APB) binds to the surface of mESC membranes readily, even in the presence of NHS-PEG-Acrylate (NPA). Even though NHS-based biomaterials usually have a greater affinity for binding to the functional groups compared to Acrylate-based biomaterials. We decided to explore and discuss this unexpected finding further in this Thesis. Similarly to NPB, we observe how APB interacts with the cell surface over the course of multiple days.

Simultaneously, we are interested in further understanding where APB conjugates on the stem cell surface; specifically, whether it binds primarily to amine or to thiol groups. The best way to address this question is to use blocking reagents. By using two different blocking reagents, one that blocks amine groups (mPEG-NHS) and another which blocks thiol groups (mPEG-Maleimide), we can investigate how the fluorescence differs compared to conditions where a biomaterial linker is added but not a blocking reagent.

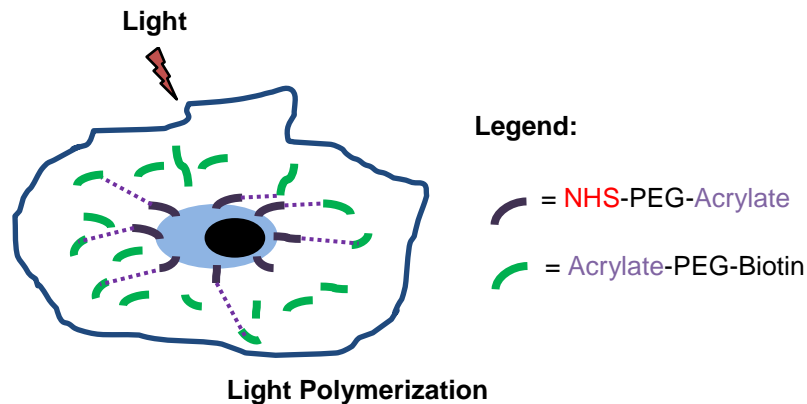


Figure 12: Schematic of modulating cell-biomaterial interactions using mESCs, acrylate domains, and light polymerization

7.2 Experimental Approach

The overall process used to label the biomaterial on the mESC surface is similar to that of the schematic in **Figure 5**. However this time, we substitute the NPB biomaterial linker with APB (MW 5000Da). Specifically, we dissolve 7.2 mg of APB powder in 250 μ L DMSO to obtain an initial concentration of 495.6 μ M. Using serial dilutions, the following dosages are obtained: 247.8 μ M, 123.9 μ M, 61.95 μ M, 31 μ M, 15.5 μ M. 123.9 μ L of each dosage is added to approximately 2.35×10^6 MEF depleted mESCs for 10 minutes at room temperature. After 10 minutes, unconjugated APB remaining in the solution is rinsed out of the system using PBS. As a control, 2.35×10^6 cells are also treated with 123.9 μ L DMSO, no biomaterial linker is added to these cells. Both biomaterial linker treated and the control mESCs are resuspended in 2.35mL of ES Media and 2.35 μ L of LIF and split for two different conditions. 1.55mL (1.55×10^6 cells) of cell suspension is used for Day 0 studies and 800 μ L (800,000 cells) replated in a well plate for next day (Day 1) studies.

Since imaging was determined to not be as sensitive of a technique as flow cytometry for our specific system, we now focus mainly on a flow cytometry based approach. Similar to previous experiments, 10 μ L of SAF647 is added to 1.55×10^6 cells in suspension for 10 minutes at room temperature in the dark. To remove unconjugated SAF647, the system is rinsed with FACs buffer. 1mL (1×10^6 cells) of the cell suspension (APB binds to both the mESC surface and to SAF647) is required for Day 0 studies. On Day 1, the cells are trypsinized from the well plates and MEF depleted once

again. 10 μ L of SAF647 is added to 1×10^6 cells for 10 minutes at room temperature in the dark. Again, unconjugated SAF647 is rinsed from the system with FACs buffer. The mESCS (1×10^6) are resuspended in 1mL of FACs buffer and used for flow cytometry. On both days, 10 μ L of Propidium Iodide (PI) dye is added to the cell suspension. PI dye is taken up by dead cells and allows one to gate around the alive cells. This will allow for better understanding and quantification of cell viability.

We also investigated the effects of blocking amine or thiol functional groups on mESC cell surfaces. The process is similar to above except we now first introduce either an amine or a thiol blocker onto the mESC cell surface. We dissolve 20mg of both the mPEG-MAL and the mPEG-NHS powders (separately) into 1000 μ L of DMSO to obtain a final concentration of 991.2 μ M for both. These blocking solutions are added to 4.7×10^6 MEF depleted mESC cells for 20 minutes at room temperature. After time is completed, remaining blocking reagents in the solution are rinsed out of the system using PBS. As a control, 4.7×10^6 cells are also treated with 1000 μ L of DMSO. The control and blocking reagent treated mESCs are both resuspended in 1.73mL of PBS and split for two different conditions (addition of APB or no addition of APB).

Specifically, we dissolve 10mg of APB powder in 1000 μ L DMSO to obtain an initial concentration of 247.8 μ M. This concentration is further diluted to obtain the final dosage of 123.9 μ M. This dosage (123.9 μ L) is added to approximately 2.35×10^6 mESCs (DMSO only control, mPEG-NHS treated, and mPEG-NHS treated) for 10 minutes at room temperature. Remaining APB in the different conditions are washed out of the system using PBS and resuspended once again in 2mL of PBS. The control DMSO only treated mESCs, 2.35×10^6 cells, receive 123.9 μ L DMSO. The steps for addition of SAF647 and mESC preparation for flow cytometry are the same as above.

7.3 Results

During flow cytometry, data is collected for 10,000 alive cells in a FSC-A vs PE-Cy5.5-A gate. To ensure that only alive cell data is analyzed at the end, the population from the FSC-A vs PE-Cy5.5-A gate is further gated with FSC-A vs SSC-A. This population is finally gated based on FSC-W vs FSC-A, thereby achieving the final desired population. The cell population from the third gating is used to draw the histograms in **Figures 13, 14, 15, and 16.**

For Day 0 studies, it can be seen that there is an incremental decrease in fluorescence/labeling as there is a decrease in the concentration of APB added into the system (from right to left in **Figure 13**). This observation is further confirmed by **Figure 14a**, where there is a greater average relative fluorescence for APB at 124 μ M than at 62 μ M when normalized to the DMSO only control. Interestingly, even at 15.5 μ M, which is 16 times less than the highest concentration in the histogram profile, the fluorescent signal is still greater than when only DMSO is added to the mESCs. Comparing fold increase in percent of dead cells data obtained from the PI dye, it is seen that the addition of APB to mESCs has only a slight increase in the percent of dead cells. This indicates that APB does not greatly affect the cells' viability negatively.

Similar to the NPB experiments, we want to observe how APB is retained on the mESC surfaces over multiple days. From general observations, it is seen that there is less mESC attachment on the MEF layer when mESCs are replated for Day 1 studies as the concentration of APB increased. On Day 0 (at 123.9 μ M), it can be seen that there is a strong fluorescent detection when compared to the DMSO only treated condition. On Day 1, there is a great decrease in fluorescence levels and the APB treated histogram overlaps with the DMSO only control histogram.

As seen in **Figure 16a and 16b**, the histograms for both the control (DMSO only) and only addition of blocking reagent (no APB) overlap and display minimal background fluorescence. Similar to before, with the addition of APB, there is an increase in fluorescence detection. In the presence of APB and both of the blocking reagents, there appears to be a minimal decrease in the fluorescence. This decrease appears to be similar for both of the conditions.

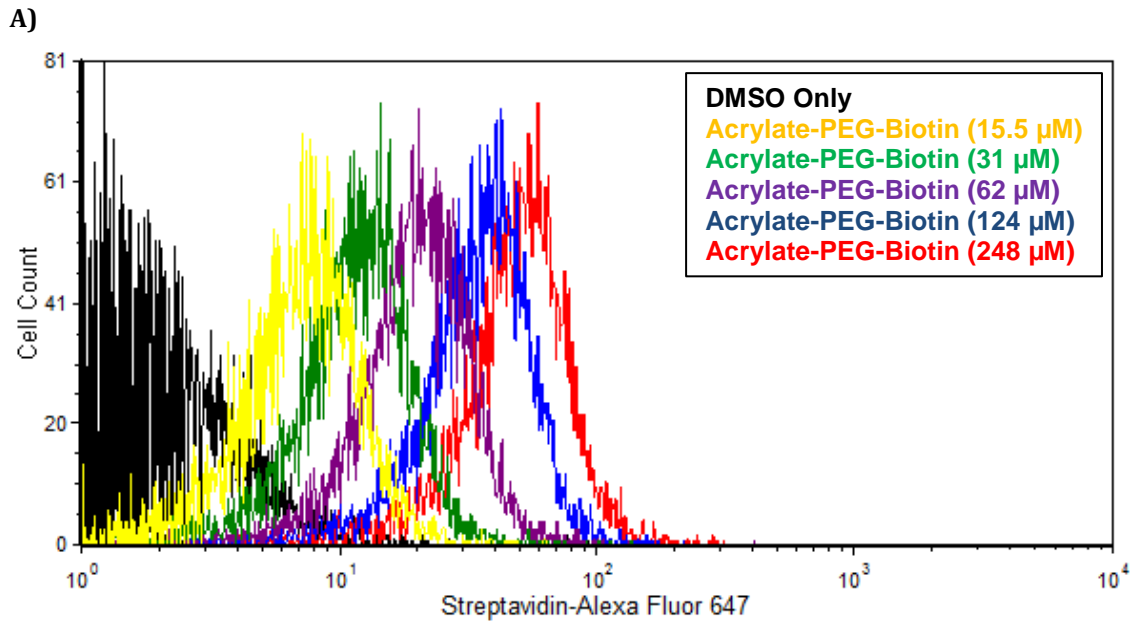


Figure 13: Similar to NPB, there is a dosage dependent decrease in fluorescence for APB on Day 0. Again, all five NPB dosages tested have a detectable fluorescence level with flow cytometry

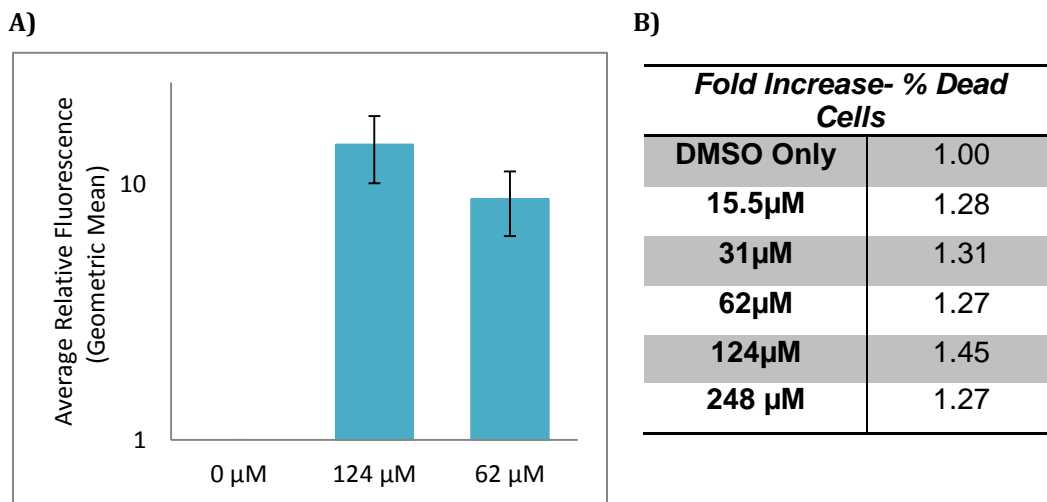


Figure 14: a) The bar graph shows a decrease in average relative fluorescence with a decrease in APB dosage on Day 0. This is similar to what is seen with the flow cytometry histograms for Day 0. b) A chart displaying a minimal fold increase in percent of dead mESCs cells with addition of APB as compared to the DMSO only control again

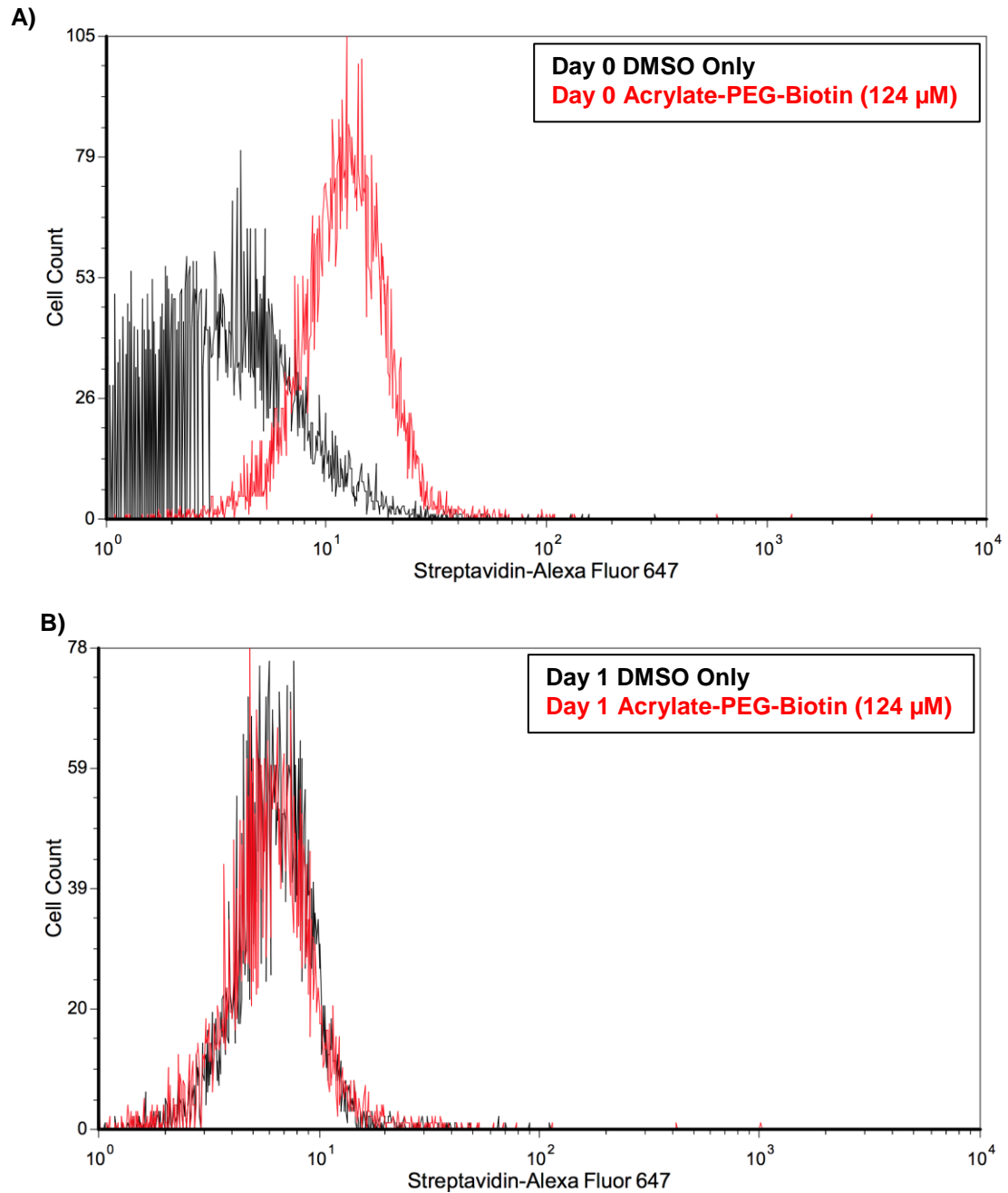


Figure 15: a) There is detectable fluorescence on Day 0 when APB is conjugated on mESC surface membranes compared to the DMSO only treated control mESCs. b) It appears that there is a decrease in fluorescence for the same APB treated mESCs from Day 0 on Day 1; the histogram overlaps with the DMSO only control. However, it is interesting to note that the DMSO only control on Day 1 has shifted towards the right compared to the histogram for control cells on Day 0 despite Day 1 control cells originating from mESCs used on Day 0

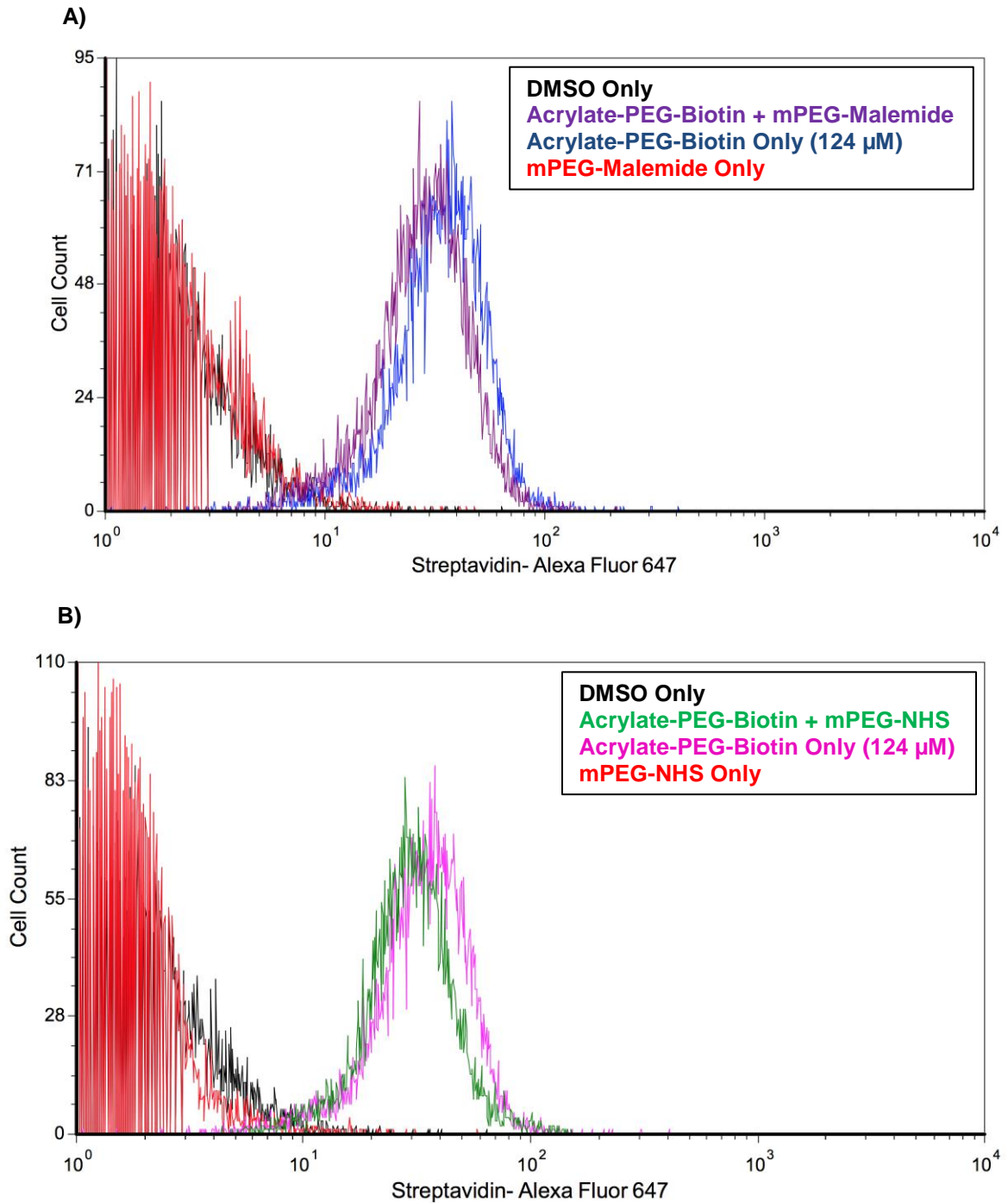


Figure 16: As seen in the histograms produced by flow cytometry, there is a slight decrease in fluorescence with the addition of the two surface blockers, a) mPEG-Maleimide and b) mPEG-NHS, to mESC surface membranes compared to fluorescence levels with the mESCs only labeled with APB. This decrease could potentially elucidate which functional group, amines or thiols, Acrylate-based biomaterials are more likely to conjugate to on mESC surface membranes

7.4 Discussion

Even though APB binds more readily to mESC surfaces, its fluorescence detection is not as strong as that of NPB, even if a similar or larger dosage is added. Although, similar to previous tests, there is a strong correlation between the concentration of biomaterial linker added to the surface and to its fluorescence detection, for both single day and multiple day studies. For APB, it appears that the highest concentration that can be on the mESC surface prior to saturating the surface is 248 μ M. Higher concentrations display a similar fluorescence profile to that of APB at 248 μ M. Using this information in conjugation with the observation of mESC attachment for multiple days, the optimal concentration for APB studies is 124 μ M.

Based on literature research, one possible explanation for the binding of Acrylate-based biomaterial linkers to the cell surface is due to the occurrence of the Michael-type addition reaction. In this reaction, various Michael donors (amines, enolates, thiols, and phosphines) can react with different Michael acceptors ((meth)acrylates, (meth)acrylamides, maleimides, acrylonitriles and cyanoacrylates) (**Figure 17**). This reaction benefits from mild reaction conditions and minimal by-product formation (Li, 2010). According to Li *et al*, it was found that to optimally accelerate the rate of this binding reaction, primary amines (in our case, amine groups located on the cell surface) act as catalysts at ambient temperatures thus producing product at a faster rate. A combination of Michael addition and photoinitiated radical curing leads to higher crosslink densities and functional group conversions (Mather, 2006). This could potentially be beneficial in the future for some applications of interest and would be interesting to study further.

Again, using a plate reader with the Biotin Quantitation assay, we find that the concentration of APB (using the data from 248 μ M) is 11.2pmol/10 μ L. Although the number of thiol groups on embryonic stem cell surfaces was not found in literature, it has been shown that endothelial and fibrosarcoma cells have at least 15 cell surface proteins that contain free thiol groups (Sahaf, 2003). There are approximately 10 proteins on the endothelial cell surface which contain closely spaced thiols and the molecular masses of these proteins varied from 13 to 153kDa. On the fibrosarcoma cell surface, there are approximately 12 proteins which contain closely spaced thiols and the molecular masses of these proteins varied from 19 to 104kDa (Donoghue, 2000).

Based on the multiple day studies, it is apparent that APB tends to leave the system pretty quickly. There is a large decrease in fluorescence by Day 1. Although, it is interesting to note that there is a shift in the DMSO only control for Day 1 studies that has not previously been seen. This indicates that there possibly is some sort of cellular surface modification occurring between Day 0 and Day 1. Potentially, this surface modification may allow SAF647 to bind to mESC surfaces without actually needing a biomaterial linker to be present. This occurrence is not clear and requires further study.

Although there is a decrease in fluorescence with the addition of the blocking reagents, this does not necessary make it clear whether APB is more likely to bind to thiol or amine functional groups. Presently, it appears that APB binds to both functional groups equally, but the fluorescence decrease is not significant enough to fully support this finding. In the future, it will be interesting to observe how the fluorescence is affected if both mPEG-Maleimide and mPEG-NHS are conjugated on the cell surface prior to the addition of APB.

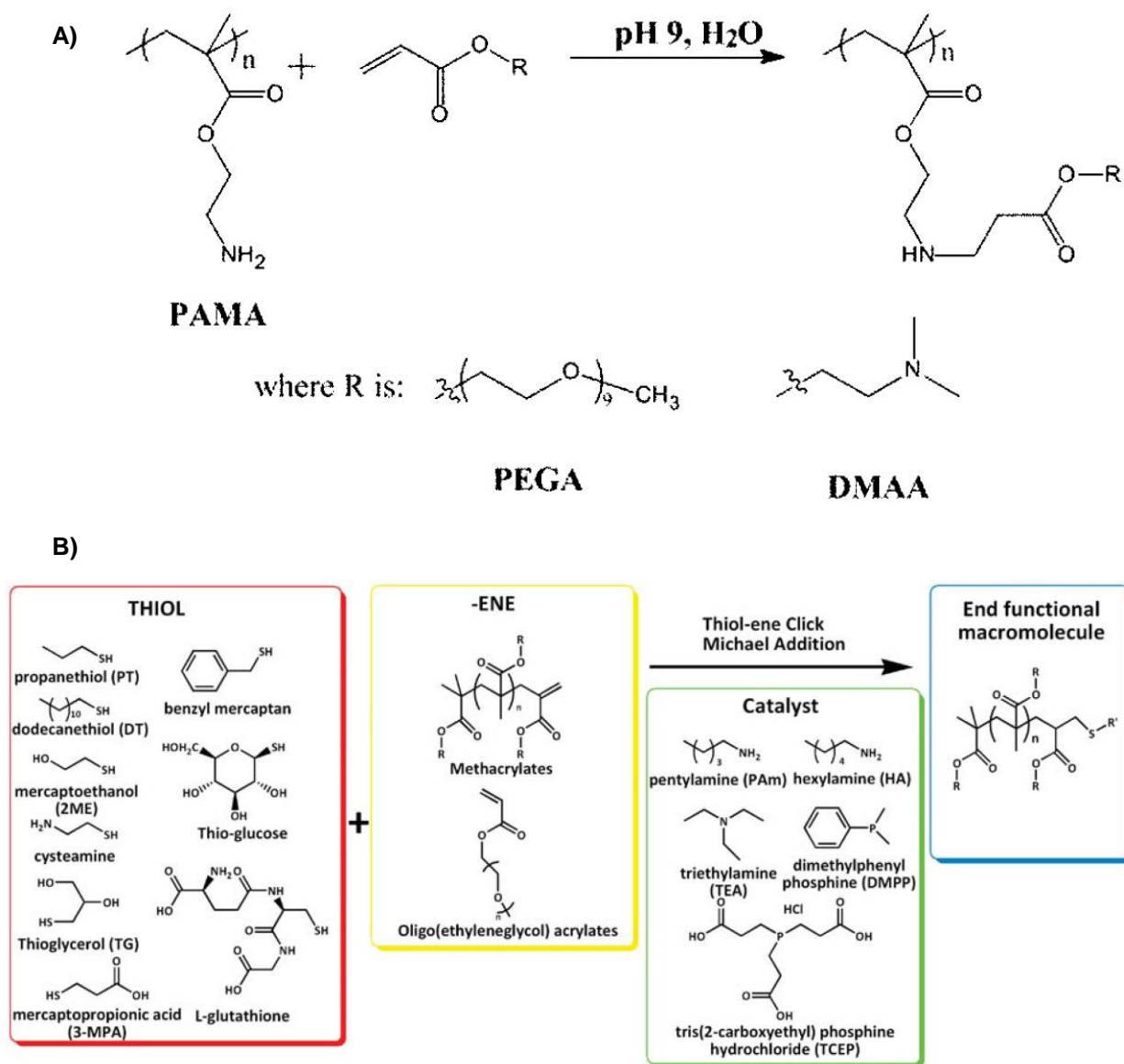


Figure 17: Michael-type addition reaction between a) an acrylate group and primary amine group (Read, 2010) and b) an acrylate group and thiol group (Li, 2010) that could potentially explain the binding of APB to cell surface membranes. In the reaction in b), amines can also potentially act as catalysts in the acrylate-thiol reaction when forming the end product; in our case, it would be the binding of the Acrylate-based biomaterial to a mESC surface membrane

Chapter 8 Conclusion and Future Directions

Currently, we have optimized both NHS-based biomaterial linkers and Acrylate-based biomaterial linkers for single day studies and only NHS-based biomaterial linkers for multiple day studies. The optimal dosage of NPB is 105 μ M while for APB, it is 124 μ M. As discussed in this Thesis, there are still some questions which remain unanswered and require further study. In terms of the Acrylate-based multiple day studies, it is clear that there is a decrease in fluorescence by Day 1, based on previous data. However, it is not clear why the fluorescence level for the DMSO only control shifts to the right. This subtle 'background signal', which was most prominent in these experiments, needs to be studied further to understand why the DMSO treated only cells are displaying fluorescence when these mESCs did not receive any other treatment. It is also important to understand the reason behind the decrease in fluorescence levels in self-renewing ES cultures through either the analysis of the loss or the partitioning of linkers with alternative methods or through optimizing a different mitotic inhibitor. The other important question to address soon is to determine what cell surface functional groups are interacting with the acrylate-based biomaterials, and in particular, if the mechanism behind their membrane conjugation could be attributed to Michael's addition reaction. Both of these questions could introduce potential new applications and may possibly affect *in vivo* studies.

As discussed, stem cell membrane engineering is a relatively new field and holds great potential for further examination and the improved understanding of various cell membrane chemistries to use in a wide range of applications. Our particular work can lead the way in understanding cell-cell interactions by integrating our specific cell membrane engineering method with photopatterning techniques, such as stereolithography, in order to pattern multilayer cellular constructs. This engineered 3D system would allow for the controlled patterning of ES cells and the introduction of spatially heterogeneous mechanical cues. Particularly, non-uniform mechanical signals within multicellular systems have been demonstrated to play significant roles in cell differentiation, proliferation, and migration which one can also investigate. This allows for the probing of complex relationship between tissue geometries, mechanical stimuli, and stem cell differentiation. Regardless of the application pursued, it is clear that the implications and potential impact of stem cell membrane engineering on tissue engineering is tremendous and one step closer to fully realized *in vivo* applications.

References

1. (2000). Tissue Engineering. *Nature Biotechnology*, 18, IT56-IT58.
2. Cheng, *et al.* (2012). Stem cell membrane engineering for cell rolling using peptide conjugation and turning of cell-selectin interaction kinetics. *Biomaterials*, 33, 5004 – 5012.
3. Cohen, D. & Melton, D. (2011). Turning straw into gold: directing cell fate for regenerative medicine. *Nature Reviews: Genetics*, 12, 243-252.
4. Donoghue, N., Yam, P., Jiang, X-M., & Hogg, P. (2000). Presence of closely spaced protein thiols on the surface of mammalian cells. *Protein Science*, 9, 2436-2445.
5. Eshghi, S. & Schaffer, D. (2008). Engineering microenvironments to control stem cell fate and function. *StemBook*, ed. The Stem Cell Research community, StemBook, doi: 10.3824/stembook.1.5.1
6. Gattazzo, F., Urciuolo, A., & Bonaldo, P. (2014). Extracellular matrix: A dynamic microenvironment for stem cell niche. *Biochimica et Biophysica Acta*, 1840, 2506-2519. doi: 10.1016/j.bbagen.2014.01.010
7. Han, Y., Wang, S., Zhang, X., Li, Y., Huang, G., Qi, H., Pingguan-Murphy, B., Li, Y., Lu, T., & Xu, F. (2014). Engineering physical microenvironment for stem cell based regenerative medicine. *Drug Discover Today*, 19(6), 763-773.
8. Jiang, X-M., Fitzgerald, M., Grant, C., & Hogg, P. (1999) Redox Control of Exofacial Protein Thiols/Disulfides by Protein Disulfide Isomerase. *The Journal of Biological Chemistry*, 274(4), 2416-2428.
9. Khire, V., Lee, T., & Bowman, C. (2007). Surface Modification Using Thiol-Acrylate Conjugate Addition Reactions. *Macromolecules*, 40(16), 5669-5677.
10. Koh, C. & Atala, A. (2004). Tissue Engineering, Stem Cells, and Cloning: Opportunities for Regenerative Medicine. *Journal of the American Society of Nephrology*, 15, 1113-1125. doi: 10.1097/01.ASN.0000119683.59068.F0
11. Kshitiz, Park, J., Kim, P., Helen, W., Engler, A., Levchenko, A., & Kim, D. (2012). Control of stem cell fate and function by engineering physical microenvironments. *Integr Biol (Camb)*, 4(9), 1008-1018.
12. Li, G., Randev, R., Soeriyadi, A., Rees, G., Boyer, C., Tong, Z., Davis, T., Becer, C., & Haddleton, D. (2010). Investigation into thiol-(meth)acrylate Michael addition reactions using amine and phosphine catalyst. *Polymer Chemistry*, 1, 1196-1204. doi: 10.1039/c0py00100g

13. Lin, C. & Anseth, K. (2009). PEG Hydrogels for the Controlled Release of Biomolecules in Regenerative Medicine. *Pharmaceutical Research*, 26(3), 631-643. doi: 10.1007/s11095-008-9801-2
14. Mahal, L. & Bertozzi, C. (1997). Engineered cell surfaces: fertile ground for molecular landscaping. *Chemistry & Biology*, 4(6), 415-422.
15. Mather, B., Viswanathan, K., Miller, K., & Long, T. (2006). Michael addition reactions in macromolecular design for emerging technologies. *Progress in Polymer Science*, 31, 487-531.
16. Medema, J. & Vermeulen, L. (2011). Microenvironmental regulation of stem cells in intestinal homeostasis and cancer. *Nature*, 474, 318-326. doi: 10.1038/nature10212
17. Metallo, C., Mohr, J., Detzel, C., de Pablo, J., Van Wie, B., & Palecek, S. (2007). Engineering the Stem Cell Microenvironment. *Biotechnol. Prog.*, 23, 18-23. doi: 10.1021/bp060350a
18. Popp, M., Antos, J., Grotenbreg, G., Spooner, E., & Ploegh, H. (2007). Sortagging: a versatile method for protein labeling. *Nature Chemical Biology*, 3(11), 707-708. doi: 10.1038/nchembio.2007.31
19. Rahman, M., Lane, A., Swindell, A., & Bartram, S. (2009). Introduction to Flow Cytometry. *ABD SEROTEC*, 1-34.
20. Read, E., Thompson, K., & Armes, S. (2010). Synthesis of well-defined primary amine-based homopolymers and block copolymers and their Michael addition reactions with acrylates and acrylamides. *Polymer Chemistry*, 1, 221-230. doi: 10.1039/b9py00320g
21. Sackstein, R., Merzaban, J., Cain, D., Dagia, N., Spencer, J., Lin, C., & Wohlgemuth, R. (2007). *Ex vivo* glycan engineering of CD44 programs human multipotent mesenchymal stromal cell trafficking to bone. *Nature Medicine*, 14(12), 181-187. doi: 10.1038/nm1703
22. Sahaf, B., Heydari, K., Herzenberg, L., & Herzenberg, L. (2003). Lymphocyte surface thiol levels. *PNAS*, 100(7), 4001-4005. doi: 10.1073/pnas.2628032100
23. Sarkar, D., Vemula, P., Teo, G., Spelke, D., Karnik, R., Wee, L. & Karp, J. (2008). Chemical Engineering of Mesenchymal Stem Cells to Induce a Cell Rolling Response. *Bioconjugate Chem*, 19(11), 2105-2109. doi: 10.1021/bc800345q
24. Stephan, M., Moon, J., Um, S., Bershteyn, A., & Irvine, D. (2010). Therapeutic cell engineering with surface-conjugated synthetic nanoparticles. *Nature Medicine*, 16(9), 1035-1042. doi: 10.1038/nm.2198
25. Stock, U. & Vacanti, J. (2001). Tissue Engineering: Current State and Prospects. *Annual Reviews of Medicine*, 52, 443-51.

26. Swiston, A., Cheng, C., Um, S., Irvine, D., Cohen, R., & Rubner, M. (2008). Surface Functionalizing of Living Cells with Multilayer Patches. *Nano Letters*, 8(12), 4446-4453.
27. Underhill, G. (2012). Stem cell bioengineering at the interface of systems-based models and high-throughput platforms. *WIREs Syst Biol Med*. doi: 10.1002/wsbm.1189
28. Underhill, G., Galie, P., Chen, C., & Bhatia, S. (2012). Bioengineering Methods for Analysis of Cells In Vitro. *Annual Review of Cell Dev. Biol*, 28, 385-410. doi: 10.1146/annurev-cellbio-101011-155709
29. Verweij, J. & Pinedo, H. (1990). Mitomycin C: mechanism of action, usefulness and limitations. *Anticancer Drugs*, 1(1), 5-13.
30. Wagner, J., Kean, T., Young, R., Dennis, J., & Caplan, A. (2009). Optimizing mesenchymal stem cell-based therapeutics. *Current Opinion in Biotechnology*, 20, 531–536. doi: 10.1016/j.copbio.2009.08.009
31. Xu, J. (2005). Preparation, Culture, and Immortalization of Mouse Embryonic Fibroblasts. *Current Protocols in Molecular Biology*, 28(1), 1-8.
32. Zhang, J. & Linheng, L. (2008). Stem Cell Niche: Microenvironment and Beyond. *The Journal of Biological Chemistry*, 283(15), 9499-9503. doi: 10.1074/jbc.R700043200
33. Zhao, W., et al. (2012). Cell-surface sensors for real-time probing of cellular environments. *Nat Nanotechnology*, 6(8), 524-531. doi: 10.1038/nnano.2011.101